MASTER THESIS

Micropatterns on Polyacrylamide Hydrogel for Controlled Cardiomyocyte Attachment using PLL-PEG and ECM proteins

Kirsten van Dorenvanck

Master Program
Biomedical Engineering

Faculty & Department
Faculty of Science and Technology
Applied Stem Cell Technologies

Examination Committee
Prof.dr. P.C.J.J. Passier
M. Catarino Ribeiro MSc
Dr. Ir. J. Rouwkema

Date
21 August 2019

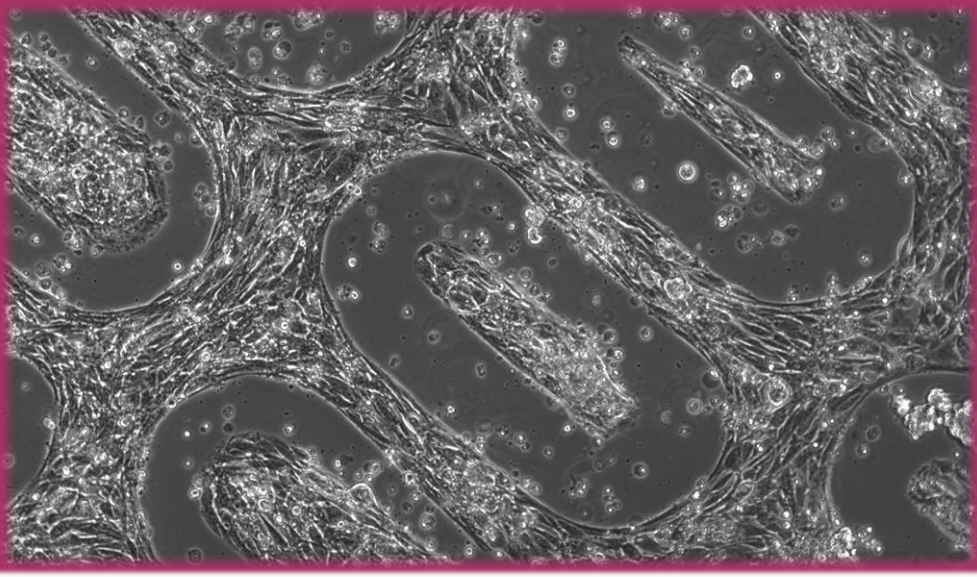

UNIVERSITY OF TWENTE.

Abstract

Poly-L-Lysine-graft-poly(ethylene-glycol) PLL-PEG and extracellular matrix (ECM) proteins can be used to create micropatterned areas for cardiomyocyte cell adhesion and surface passivation on polyacrylamide (PAA). This research endeavoured to optimize a protocol designed to create these cell micropatterns using several combinations of PLL-PEG and ECM cell adhesive proteins vitronectin, fibronectin, gelatin, and gelatin-methacrylate (gelMA). Vitronectin, fibronectin and gelatin were used as a coating, where gelMA was mixed in the PAA. The results for the cell micropatterns were inconsistent, with identical or similar methods giving either no, correct, or inverse micropatterns. The most consistent and correct micropatterns were found for the use of PLL-PEG and PAA-gelMA. The highest quality of micropatterns was found for PLL-PEG and gelatin on PAA, however, these patterns were inverse. Furthermore, the removal of excess PLL-PEG after coating was found to increase micropattern overall quality. Additionally, some minor protocol optimizations were made.

Table of Contents

Abbreviations

The abbreviations used in this thesis are here mentioned in order of use.

CVD	cardiovascular disease
hESC	human embryonic stem cells
hiPSC	human induced pluripotent stem cell
PAA	polyacrylamide
APS	ammonium persulfate
TEMED	tetra-methyl-ethylene-diamine
PDMS	polydimethylsiloxane
ECM	extra cellular matrix
RGD	arginine-glycine-aspartic
gelMA	gelatin-methacrylate
PEG	poly (ethylene glycol)
PLL	poly-L-lysine
PLL-PEG	poly-L-lysine-graft- Poly-(ethylene glycol)
UV	ultraviolet
hESC CMs	human embryonal stem cell derived ΔN3 Coup-red cardiomyocytes
Draggn CMs	Draggn-3A1-nkX 2.5 GFP-Actin-mRuby cardiomyocytes
FITC	fluorescein isothiocyanate

1 Introduction

1.1 Cardiovascular disease

Yearly in Europe, cardiovascular disease (CVD) causes around 3.9 million deaths, making it the leading cause of death in 12 European countries. CVD accounts for 45% of all deaths in Europe and is estimated to cost the EU economy €210 billion a year.[1] CVD generally refers to conditions with the heart muscle, valves, rhythm, or blood vessels. One of the issues with CVD is that the cardiomyocytes, the heart muscle cells, have a low proliferative capacity. This makes the healing of the heart problematic, as cardiomyocytes make up around one-third of the cell number in the heart, and 80-90% of the volume of the myocardium. [2] The loss of cardiomyocytes that happens after heart damage means the other working myocytes need to compensate for the workload. [3] Next to the loss of cardiomyocytes, the healing of the heart is mostly done by creating scar tissue made out of non-myocyte heart cells, of which most are cardiac fibroblasts and fibrillar collagen. This scar tissue often elevates the risk of arrhythmogenesis and heart failure, due to the scar's inability to transmit electrical signals or contract. [4, 5]

To alleviate the risks of such complications and improve the heart's condition, medicinal drugs can be used. Current often applied medications are antiplatelets to prevent blood clotting, statins to protect blood vessels, or beta-blockers to reduce the heart's workload. However, these often-used treatments only offer limited protection from further heart disease and limited improvement of heart function. Next to this, drugs often have side effects, and when combined together these side effects may increase, or even interact negatively.[6] Therefore there is a need for new and improved medicine for CVD to improve the heart function and lower risks of further complications, with less or even no side effects.

The goal of this research is therefore to improve and optimize a protocol based on the research done by Vignaud et al, to create the prospect of a high throughput assay using micropatterned cardiomyocytes on polyacrylamide hydrogel for drug development. [7] The micropatterns are created using cell adhesive ECM proteins and PLL-PEG, an anti-fouling protein.

1.2 Drug development

The discovery of new drugs for any disease is a large field of research, and the most important part of the drug is its safety and t therapeutic effect. Therefore, drug discovery requires multiple studies with *in vitro* and *in vivo* research. Up to 30% of all potential new drugs are cancelled due to unexpected side effects or inefficiency and failure of the pre-clinical tests, where the false positive rate is estimated to be as high as 25%. In addition to this difficulty with drug development, many drugs have side effects on heart cells due to their toxicity to the cell. This is called cardiotoxicity. The cardiotoxicity of drugs is difficult to observe and sometimes missed in *in vitro* and *in vivo* models. *In vitro* models do not compare to the human body, as the body gives a specific surrounding for the cells with communication, proteins and specific tissue anatomy, which lacks for *in vitro* models. *In vivo* models often start with the use of rodents, building up to larger animals with success of the tests. However, these models are not accurate for the human body, as they can behave differently to the drug for toxicity, efficacy, and side effects. [8, 9] This results in the need for better drug testing models and assays with the use of adult cardiomyocytes.

The use of human adult cardiomyocytes is limited, due to the non-proliferative nature of the cells. They can only be directly obtained by the use of a donor. However, the amount of donors is limited, which poses a new problem for the acquirement of these heart cells.[10] This problem can be overcome by the use of stem cells. Human cardiomyocytes can be differentiated from human embryonic stem cells (hESCs), or human induced pluripotent stem cells (hiPSCs). hESCs are a type of pluripotent cells that can bring about all somatic cell types in the embryo, and have the ability for indefinite renewal. With the

correct cues, they can be guided to differentiate into any desired cell type. However, hESCs can only be obtained from early-stage embryos, leading to many ethical debates and controversy about their use. [11, 12] hiPSCs are de-differentiated somatic cells, brought back to pluripotency similar to the hESC, including the self-renewing properties. These cells overcome the difficulties that arise with the use of hESCs.

By using hiPSC derived cardiomyocytes, patient-specific cell lines can be used for a more specific and personalized perspective of drug development. However, the cardiomyocytes obtained by this method often show difficulty in becoming adult cardiomyocytes, showing signs and function of immature cardiomyocytes. Several methods to create adult cardiomyocyte are currently being researched, including the use of small molecules, long term culture, mechanical loading, culture substrate, environmental manipulation, cell alignment, and 3D cell growth methods. [13-21]

1.3 Cardiomyocyte function in drug development

Three of the major cardiomyocyte properties that are influenced by drugs are contractile strength, contractile rhythm, and viability of the cells. The aim of cardiac drugs is to normalize these parameters for the human body, regaining the original function of the heart. It is therefore important to quantify these parameters. [22]

The contractile strength of a cardiomyocyte is here separated into two properties; internal and external contraction. The former is the internal force generated by the cell during contraction, created by the contraction of myofibrils in the cell. The latter is defined as the effect of the generated force of the contracting cell on the displacement of its surroundings, be it in a tissue or on a substrate.

Depending on the substrate the cardiomyocyte grow on or in, the internal force generation of the contracting cell may not translate completely to the substrate. In other words, the internal contraction of the cell does not have to be equal to its external contraction. This depends on the stiffness of the substrate. In the heart, stiffness of healthy myocardial tissue is between 10 to 30 kPa, whereas after for instance a stroke can increase up to 150 kPa. With a lower stiffness, the substrate moves more easily with the internal contractile force of the cardiomyocyte. With an increasing stiffness, there is a point where the cardiomyocyte is unable to displace the substrate at all. [23] Substrate stiffness also affects other properties of cardiomyocytes, such as maturity, morphology, gene regulation, and cell electromechanical coupling, which are all aspects of cardiomyocyte health and function. [24] Many cell cultures are currently done using rigid tissue culture polystyrene, which has a stiffness of roughly 1 GPa, which is much more rigid than the matrix the cells naturally grow in. Using a substrate for cell culture which mimics the native biological stiffness will give results that show more accurate representation for the body. [25]

Internal contraction is often measured using fluorescent dyes or reporter lines of cardiomyocytes with for instance fluorescently tagged sarcomeric proteins. With these dyes, cell displacement and contraction frequency can be easily measured *in vitro*. [26, 27]

External contraction is shown to be measured by the use of magnetic beads, polyacrylamide gels, carbon fibre deflection, atomic force microscopy, optical edge detection, flexible cantilevers, micropost arrays, and strain gauges. These methods use either the measurement of displacement or force of the substrate or measuring instrument. [28] New contractile force measurements are still being developed. [19, 29]

In recent research, both internal and external force was measured *in vitro* by the use of fluorescently tagged cardiomyocytes, and fluorescent beads in a polyacrylamide hydrogel. [30] This is one of the methods that can be applied in the context of the research done here.

1.4 Polyacrylamide as a cell culture substrate

As previously mentioned, the substrate on which the cardiomyocytes grow is vital to cell health and behaviour. Polyacrylamide (PAA) is a biocompatible hydrogel that has been widely used for a number of studies concerning cell culture substrate stiffness. PAA can be made in a wide range of stiffness, from 0.010 to 50 kPa, by mixing a ratio of acrylamide monomer and bis-acrylamide crosslinker in the presence of ammonium persulfate (APS) and tetra-methyl-ethylene-diamine (TEMED), as shown in figure 1. APS is the source of free radicals required, while TEMED acts as a catalyst to initiate the redox radical polymerization. Thin layers of PAA are often used on a rigid substrate, such as a cell culture plate, or a glass coverslip. This rigid surface can be coated with aminosilanes to attach and immobilize the PAA hydrogel to the surface. [25, 31-33]

PAA is bio-inert, having no cell surface receptors or cell interaction. Therefore, no cell attachment occurs unless protein conjugation to the PAA hydrogel surface is used to enable this. A coating of cell adhesive proteins can also be used to promote cell attachment. PAA is optically transparent, making it possible to observe through the gel. A disadvantage of PAA is that it cannot be used for 3D culturing, as it cannot encapsulate cells due to the toxicity of the precursor materials. [33]

To track external cardiomyocyte contraction, fluorescent beads can be mixed in the acrylamide solution prior to polymerization. The amount of contractile force the cells then create on the PAA is translated to a displacement in the fluorescent beads, which can be measured.[30] Together with the tailoring of the PAA stiffness, this creates a good way of measuring external cardiomyocyte contraction force *in vivo* on different stiffnesses, while keeping the capability to also measure the internal contraction of the cells. Therefore PAA is used in this research.

1.5 Cardiomyocyte alignment and micropatterns

The norm in cell culture is the use of a 2D surface, whereupon cells can be seeded and cultured. This can result in a monolayer of cells, single cells, or groups of cells attached together. This, however, does not simulate the situation in the body, where cells grow in a specific alignment, structure and organization. This same situation goes for cardiomyocytes in the human heart. [34]

Adult human cardiomyocytes naturally have the dimensions of 10 to 20 µm in width, with a length of 80 to 100 µm, creating a rod-shaped cell. [35] In contrast to skeletal muscle cells, adult cardiac muscle cells contain two nuclei. They contain a lot of mitochondria and much myoglobin due to the high requirement of ATP through aerobic metabolism. They also show much branching and connect end to end through intercalated discs, creating a three-dimensional network of cells that can contract simultaneously in length for optimal contraction. This structure makes up a large part of the myocardium, one of the three layers of the heart wall [36-38]

In a 2D culture, this conformation of cells translates to a unidirectional alignment of cardiomyocytes, instead of the random growth patterns otherwise seen in 2D culture. Creating this alignment requires direct control over the spatial organization of cells at µm scale. This control can guide not only the organization, but also cell fate and function. Setting boundary conditions in cell culture on microscale can give this control and is called micropatterning.

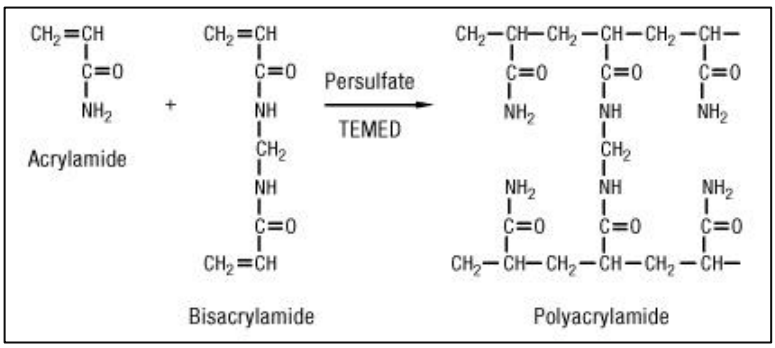

***Figure 1**: Polymerization of polyacrylamide using acrylamide, bis-acrylamide, ammonium persulfate, and TEMED. Source from Thermofisher on polyacrylamide gels.*

Creating these micropatterns in cell culture has been much researched upon, and this has

resulted in several methods of obtaining this cell alignment. The methods used for this can be divided into several subsections: Surface topography engineering, patterned cell deposition methods, or chemical surface engineering.

Surface topography engineering methods use the surface properties of the substrate for specific alignment or patterning of cells. For instance, a grooved surface can elongate and align cells according to the width of these grooves.[39] In similar research, wavy patterns were used to create increased alignment and adhesion strength.[40] Porosity and rigidity are also factors that affect cell attachment, although these methods are often used together with chemical surface engineering for optimal cell patterning. [41]

Patterned cell deposition methods use a cell seeding method that allows for the very precise deposition of cells onto a surface. Amongst these methods are photo- and soft lithography, which use stamps often made of Polydimethylsiloxane (PDMS) to deposit cells onto a surface with an accuracy of up to 1 µm. PDMS stamping is limited by the type of material that it can stamp onto. Bioprinting in all its variants is also widely used, with the newer 3D bioprinting that can deposit cells in a bio-ink onto a surface, building layers of this bio-ink as it moves in the x, y and z-direction using a nozzle. [42-46] These methods require specialized equipment, which is often not readily accessible in laboratories, as well as extremely precise protocol optimisation to create reliable and reproducible results. [47]

The most used methods are in the category of chemical surface engineering. Chemical surface engineering has been used to increase or decrease cell attachment, promote (de)differentiation, or change the surface properties such as hydrophobicity/hydrophilicity, charge, etc. [48] Other techniques include the use of plasma-treated PDMS surfaces, general micromachining-like techniques, or photopatterning light-sensitive materials. [49-51]

A more common method uses the controlled deposition of extracellular matrix (ECM) ligands, a type of cell adhering molecule. This method is applied to guide single-cell morphology when used on a small enough scale. [52] This method of applying adhesive molecules onto a surface to promote specific cell attachment is widely used, often with ECM matrix proteins such as fibronectin, laminin or collagen. These molecules are preferable to cell attachment compared to the glass or plastic surfaces used in cell culture. [53] The exact deposition of these ECM proteins onto a surface in the desired micropattern is often done in a similar fashion as for the previously mentioned patterned cell deposition methods; different types of lithography, or microcontact printing. One such method is similar to the previously mentioned photopatterning. A similar method uses a technique called the lift-off microtechnology. This method creates a sacrificial layer, in which inverse patterns are etched using UV light. The non-etched areas are washed away, and a cell adhesive (or non-adhesive) protein is coated on the entire surface. What is left of the etched sacrificial layer is then removed using a soluble, taking the coating on top of this inverse pattern with it, and leaving the desired pattern of cell adhesive (or non-adhesive) protein behind. [54]

1.6 Cell Adhesive Proteins

The micropatterning methods used in this research are mostly chemical surface engineering, with the use of cell adhesive and anti-fouling proteins. Therefore, more insight is given on the properties and possibilities of these proteins.

The natural matrix in the body that cells grow in contain a mixture of molecules that controls the integrity, function, and spatial organisation at the cell surface and in-between cells. This matrix is called the ECM. The molecules responsible for cell-cell and cell-tissue matrix interactions are called cell adhesion molecules. Cell adhesion proteins can be divided into 6 categories. Of these categories, 4 are based on protein-protein interaction, and 2 involve protein-carbohydrate interaction. The four based on protein-protein interaction are; the immunoglobin superfamily, cadherins, integrins, and receptor protein

tyrosine phosphatases. Protein-carbohydrate categories contain selectins and hyaluronate receptors.[55-57] Apart from these proteins, peptides can also be used to promote cell attachment, spreading, and viability. [58]

Of these categories, all but the hyaluronate receptors involve cell-cell adhesion. Integrins and hyaluronate receptors are the ones involved in cell-matrix interactions. These cell-matrix proteins promise to be the most effective for this research, as specific cell alignment and patterning to a substrate is the desired outcome. [55, 59] Hyaluronate is mostly used for tissues such as cartilage, and is therefore of little use for this research. [55]

Integrins are transmembrane cell receptors, containing one α and one β chain required for cell-cell or cell-matrix interactions. Three subfamilies of integrins exist; β1, β2 and β3. The β1 and β3 families regulate cell-matrix interaction, while β2 contains cell-cell adhesion molecules mostly limited to leucocytes. The difference between β1 and β3 is that β1 integrins involve adhesion to connective tissues and macromolecules. This contains ligands like fibronectin, laminin and collagen. The β3 integrins involve adhesion to vascular ligands, such as fibrinogen, von Willebrand factor, thrombospondin and vitronectin. Clusters of these integrins on a cell create areas called focal adhesion sites. [55, 60-62] Of these proteins fibronectin, vitronectin, and collagen-derived gelatin are used in this research as cell adhesive proteins, and will therefore be explained more in-depth.

Vitronectin, a protein belonging to the adhesive glycoprotein group, is responsible for attachment of cells to the surrounding matrix. It is also known to promote cell differentiation, proliferation and morphogenesis. Vitronectin is naturally found as a plasma protein, although it is also shown to be present in tissues under pathophysiological conditions. The natural concentration of vitronectin in plasma is between 200 and 400 μg/mL, which is around 0.2 and 0.5% of the total proteins found in the plasma. Another vitronectin source is contained in platelets for rapid release. The amount of this vitronectin is around 0.8% of the total vitronectin in the human body. Vitronectin has a molecular mass of 75 kDa, and an isoelectric point of between pH 4.75 and 5.25. The protein is established to bind to the cell membrane integrins αvβ3, αvβ5, αvβ1 and αIIbβ3. Of these integrins, αvβ3 and αvβ5 show to promote cell spreading, migration, and attachment.[63]

Fibronectin has a variety of interaction with the natural extracellular matrix, including important interactions with cell adhesion. It is a dimer consisting of two near-identical subunits of around 250 kDa, covalently linked near the C-termini by disulphide bonds. The concentration of fibronectin found in plasma is roughly 300 μg/mL, and it has an isoelectric point of within the range of pH 5.6 to 6.1. Fibronectin is a ligand for many integrin receptors. The most used fibronectin receptors are α5β1, α4β1, and α4β7. Fibronectin is also capable of binding to biologically important molecules such as heparin, collagen/gelatin, and fibrin. [64, 65]

Collagen is a protein found in all vertebrates and provides mechanical stability for tissues. It creates a functional environment for cells. Depending on the tissue and its physical properties, collagen 1 fibrils made of a triple helix are found in different arrangements and diameters. Narrow fibrils are found in the cornea where optical transparency is required, and large-diameter fibrils are found in tendons for the use of high tensile strength. [62, 66] The isoelectric point of collagen depends heavily on the pH. Integrins with the domain subunits α1, α2, α10 and α11 are considered to be the main groups of collagen receptor integrins. All collagen receptor α subunits contain a common β1 subunit. This allows cells to bind to collagen. Many other proteins can also bind to collagen. Many collagens are also recognized by receptors that also bind to fibronectin and vitronectin. [62, 66, 67]

Gelatin is a heat-denaturated form of collagen. Its charge depends heavily on pH, as it does for collagen, and has an isoelectric point of pH 7.0-9.0 for type A, or between pH 4.7 and 5.4 for type B. At pH values lower than the isoelectric point, gelatin has an overall positive charge. The triple-helical formation that

is present in collagen unfolds during heating and forms random coils instead.[68] This creates a less ordered macromolecular structure.[62] Collagen receptor integrins do not recognize this protein. However, new integrins such as α5β1 and αV are now able to bind to gelatin. These integrins are also able to bind to vitronectin and fibronectin.[67] Gelatin also contains many arginine-glycine-aspartic acid (RGD) sequences. These sequences also promote cell attachment. Gelatin is different than collagen in that it is better soluble, and has less antigenicity.[62, 69]

Gelatin methacrylate (gelMA) is a hydrogel that is photopolymerizable by the addition of methacrylate. GelMA is synthesized by the addition of methacrylic anhydride to gelatin at 50°C. The addition of a UV sensitive molecule like Irgacure 2959 allows for the photopolymerization process. The main benefit of gelMA over gelatin is that gelMA is stable at higher temperatures, as gelatin becomes liquid at 37°C, a standard temperature used in incubators for cell culture, while gelMA stays solid and keeps its mechanical properties. The RGD motifs are not significantly influenced by the synthesis of gelMA, and therefore the cell adhesive properties are retained. GelMA is often used in 3D culture, or when a stable cell culture substrate is required. With the use of collagenase, it is possible to degrade the hydrogel if required. [69-71]

1.7 Anti-fouling molecules

Opposite to creating cell adhesive surfaces for the use of micropatterns, using anti-fouling surfaces to create non-adhesive areas is just as important to create defined, clear micropatterns for cell attachment. The areas where cell attachment is undesired can be made or coated with an anti-fouling protein or other molecule or material, preventing cell adhesion while not causing cell damage or cell death and maintaining biocompatibility. Not only do anti-fouling surfaces repel cell adhesion, but they often also prevent other protein interactions with the surface. These proteins mediate further biofouling of the surface, including contamination of the surface by bacteria, fungi and viruses. [72-74]

Surface hydrophobicity, non-adhering materials such as ceramics, metals or specific polymers, and sophisticated materials to obtain specific cell adhesion have been used to create the desired cell adhesive properties. However, when a substrate with specific mechanical properties is required which does not have the ideal cell adhesive properties, the surface properties of this substrate need to be altered instead. This requires additional materials to create the desired surface properties. [75, 76] Surface grafting of poly(ethylene glycol) (PEG) has shown to be the most reliable and efficient approach to create non-fouling surfaces by immobilizing the PEG on a surface and has been widely accepted as the best surface anti-fouling material. The use of PEG is favourable for anti-fouling due to its inertness properties; hydrophilicity, flexibility, and lack of charge, and steric repulsion due to chain compression in water. This coating can be done by physical adsorption, chemical adsorption, direct covalent attachment, and block or graft copolymerization. However, physical adsorption and covalent attachment of PEG is limited by steric hindrance, meaning that with an increase in PLL-PEG coating density, there is a decrease of PLL-PEG addition to this coating. [76-79]

The addition of functional groups to PEG is required for surface immobilization. By adding terminal amino groups or carboxyl groups, various biomolecules such as heparin, lactose, lysine, and antibodies can be bound to PEG, allowing the new PEG conjugate to bind to surfaces such as gold, resin, polyurethane, glass, or PDMS. Many studies have been done to create new PEG conjugates for different surfaces and applications. [76]

Other strategies of using PEG to coat surfaces include, but are not limited by; star-shaped chains, adsorption of block copolymers, surface-initiated polymerization, patterned brush coatings, microscopically thin hydrogels, clickable nanogels, and deposition of preformed hydrogel particles. [80]

An easy and efficient graft polymerization method of PEG coating is the use of Poly-L-lysine-graft-poly(ethylene glycol) (PLL-PEG), which can be directly adsorbed to a surface. This is done by negatively charging a substrate by oxidizing it using plasma treatment. The positively charged backbone of poly-L-lysine (PLL) then binds through electrostatic attraction to this substrate, creating a PEG top layer. A schematic view of this method can be found in figure 2. [81, 82] A PEG graft with a similar protein to PLL, such as poly(ethylene imine) would give similar results. [77] The density of the PEG on the polymer backbone and the length of the PEG determine its efficiency. A facial density of 0.1 PEG chain per nm^2 is required for efficient protein adsorption prevention. A grafting ratio of 3.5 to 5 lysine units per PEG chain was found to be optimal. [77, 83]

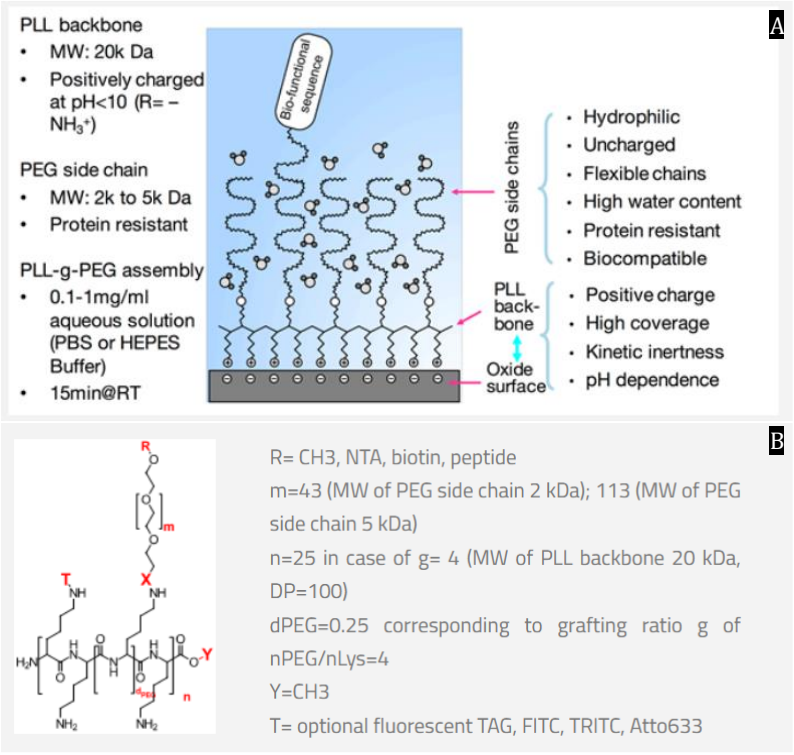

***Figure 2**: The PLL-PEG molecule and use by SuSoS. A: Schematic view of a PLL-PEG coating on an oxidized surface. B: The PLL-PEG molecule with optional modifications.*

1.8 PLL-PEG with ECM adhesive protein micropatterns on Polyacrylamide

In 2010, a combination of the above-mentioned techniques was used to create protein micropatterns. This method was designed by Azioune et al, who designed an ultraviolet (UV) photomask to create single-cell micropatterns. The photomask was used to oxidize patterns into a coating of PLL-PEG, an anti-fouling molecule. The patterns created in the PLL-PEG were coated with fibronectin, to create cell adhesive specific micropatterns in an antifouling environment. The quality of the micropatterns is limited by two factors. One is the resolution of the photomask, which is limited by the fabrication. Usually, the quality can lead up to a fraction of microns. The other factor that limits the resolution of micropatterns is the contact between the photomask and the substrate. This contact can be improved by using either a vacuum or a water drop. [84]

Vignaud et al in 2014 improved on this technique by transferring similarly created patterns onto PAA. Micropatterns were created using deep UV radiation through a photomask on PLL-PEG. A cell adhesive protein coating was then incubated on these micropatterns to create dedicated cell adhesive and antifouling areas. These micropatterns were then transferred onto PAA by polymerizing the acrylamide between the micropatterned surface and a silanized glass surface. The silanized coverslip immobilizes the PAA while transferring the micropatterns from the original coverslip to the hydrogel. A schematic view of this protocol can be found in figure 4, which describes the steps visually. [7]

The use of PAA in this method allows for the addition of another previously mentioned method; the use of fluorescent beads in a hydrogel for the measurement of the external contractile force of cardiomyocytes on a substrate. [30] Combining all these methods creates a situation where cells can grow in a controlled, patterned environment, where shape, alignment and substrate elasticity can be tailored, while simultaneously measuring internal contraction of the cell using fluorescently tagged cell strains, and measuring external contraction force on the PAA substrate by the use of fluorescent beads. This method shows great potential for the use of drug development and testing, as it allows for the testing on a substrate that can mimic the stiffness of regular or patient-specific myocardium. It can measure the function, health and maturity of the cardiomyocytes, be it adult human cardiomyocytes from a donor or cardiomyocytes derived from hiPSCs.

The protocol created by Vignaud et al. is originally used for round coverslips with a diameter between 13 and 17 mm. The throughput of this method is suboptimal, with only a limited amount of micropatterned coverslips that can be made at the same time. By upscaling this method to a 96 well plate, the throughput of micropattern creation and use would be increased significantly. This increase shows great potential for the use of assays on for instance cardiomyocyte toxicity or drug development. Next to that, this method shows easy implementation and reproducibility, without the need for specialized equipment. It is low cost, has compatibility for high throughput, and the ability to produce long-lasting µm precise micropatterns.

To produce this upscaling, a quartz photomask was designed to create micropatterns that fit the dimensions of a 96 well plate. The photomask is designed with wafers of micropatterns, as shown in figure 3. One wafer fits a 96 well exactly, and the wafers are repeated so each well has one wafer. A wafer consists of micropattern parts. Many different micropattern parts were created to test the efficiency of micropattern creation, resolution and quality of the micropatterns, and effect of the patterns on cell alignment and contraction.

Using this photomask, a large well plate-sized glass coverslip can be used to create micropatterns on in the fashion of the protocol used by Vignaud et al. [7] After creating these micropatterns, the micropatterned coverslip can then be glued to a bottomless well plate, becoming the surface on which cell culture can be performed.

Before this upscaling can be attempted, the micropatterning protocol with the use of this photomask is first to be optimised. The purpose of this research is the optimisation of this protocol, where different variants of the original protocol are tested to create well defined and reproducible micropatterns on PAA.

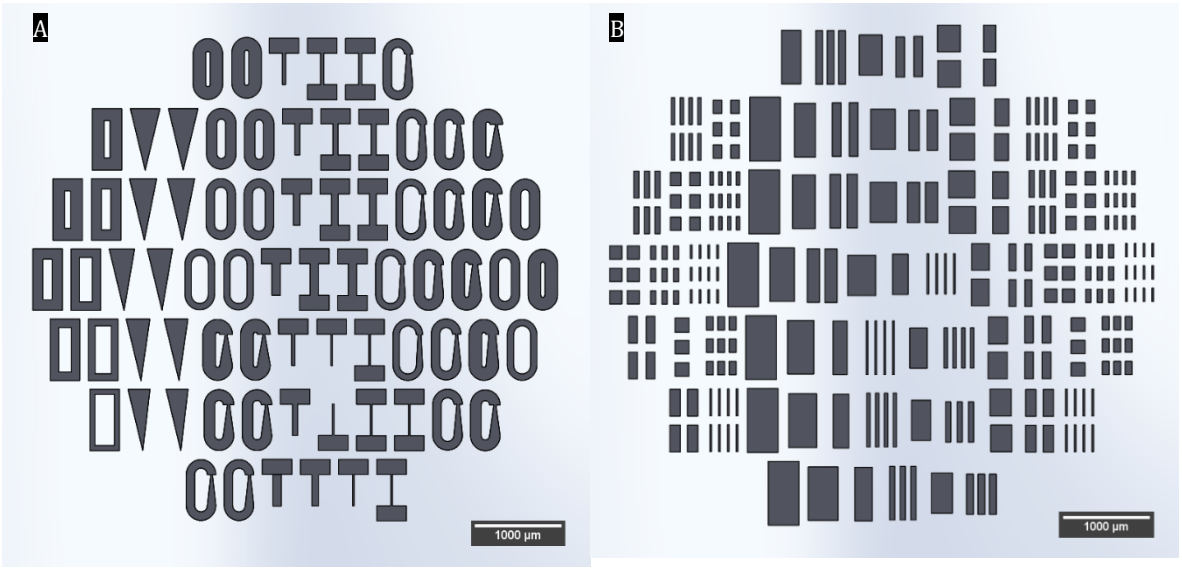

Figure 3: *The two types of wafers (A and B) are repeated in the photomask at a 96 well plate spacing distance. The micropattern parts (A) or groups of smaller parts (B) are all made in areas with maximum dimensions of 700x350 nm.*

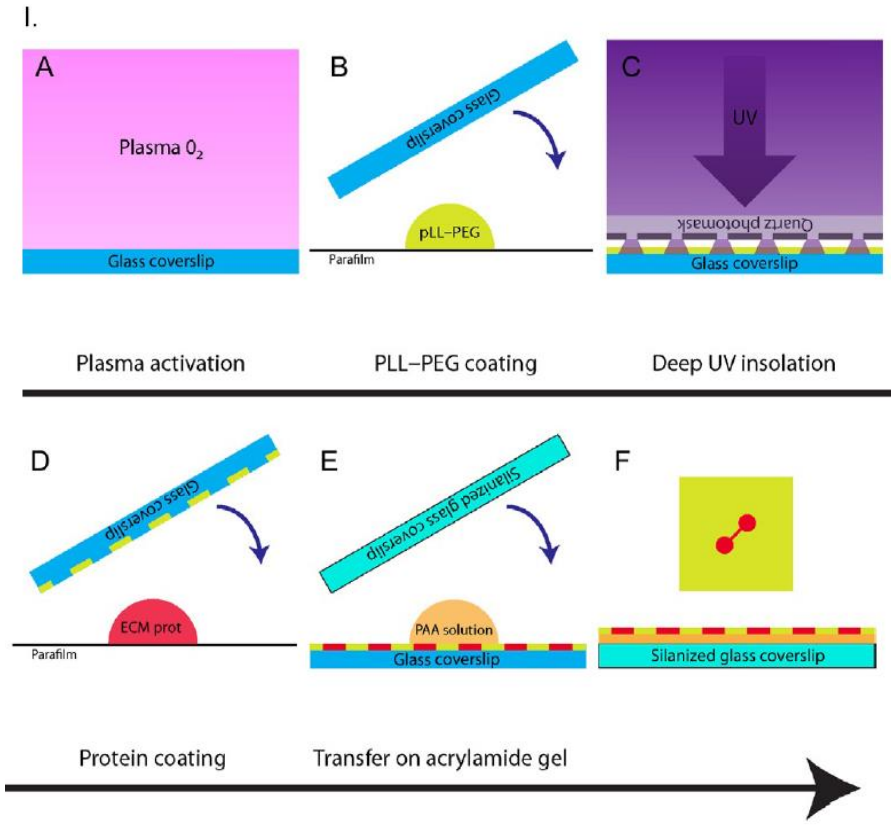

Figure 4*: original protocol designed by Vignaud et al. A: Plasma treatment of the glass surface to negatively charge it. B: PLL-PEG coating of the glass. The positive PLL tail binds to the negatively charged glass during incubation. C: micropatterning of the PLL-PEG using UV light trough a patterned photomask. D: ECM protein adsorption in the UV activated patterns. E: PLL-PEG and ECM protein transfer to PAA during polymerization and separation of the coverslips. F: Final product of micropatterns with specific cell adhesive and anti-fouling areas.*

2 Materials & Methods

2.1 Materials

The materials used in the experiments described in chapter 2.2 are listed here, ordered chronologically as used in the protocols.

Tweezers; glasswork; Parafilm; MilliQ; dH2O; Round coverslips 18 & 25 mm diameter; Coverslip rack wash-n-dry, Sigma Aldrich; Ethanol; Acetone; sonicator 1510, Branson; PLL(20k)-g3.5-PEG(2K), SuSoS; PLL(20k)-g3.5-PEG(2K) FITC, SuSoS; CUTE plasma treater, Femto science; HEPES 10 mM in MilliQ, pH 7.4, from dry powder, Sigma Aldrich; Custom quartz micropattern mask; UV/ozone procleaner plus, bioforce nanosciences; vitronectin, Thermo fisher; Fibronectin from bovine, Sigma Aldrich; Fibronectin FITC; Gelatin from porcine skin, Sigma Aldrich; Gelatin FITC; PlusOne bind-silane, GE healthcare, life sciences; Acetic acid; 40% acrylamide solution, Bio-Rad; 2% bis solution, Bio-Rad; HEPES 200 mM in milliQ, 8.2 pH, made from dry HEPES powder, Sigma Aldrich; Ammonium persulfate 10% w/w in milliQ, Sigma Aldrich; TEMED, Sigma Aldrich; gelMA obtained from dr. I. Allijn, university of Twente, TNW-BST; Dow corning vacuum grease; scalpel; centrifuge 5424 R, Eppendorf; hESC derived cardiomyocytes; Draggn-3A1-nkX 2.5 GFP-Actin-mRuby cardiomyocytes; CM medium with Galactose, low insulin; Glucose; Triiodo-L-Thyronine (T3) thyroid hormone, Sigma Aldrich; LONG® R3 IGF-I human, Sigma Aldrich; HCL 5 M; RevitaCell, Thermo fisher; dPBS-/-, Thermo fisher; TrypLE, Thermo fisher; DMEM, Sigma Aldrich; Nikon Eclipse TE2000 inverted microscope located inside a humidified incubator (used for fluorescent images); Nikon eclipse ts2-fl diascopic and epi-fluorescence illumination microscope (used for brightfield images).

2.2 Original protocol

Described here is the protocol taken as the initial baseline for this research. It is a slightly adapted protocol based on the protocol designed by Vignaud et al.[7] The protocol is divided into segments for an easy overview and reference. A visual representation of the process can be found in figure 4. Further methods are adaptations of the original protocol. If no changes are made to the protocol, the corresponding segment is referred to as the method. Changes of the original protocol will be explicitly mentioned.

2.2.1 Coverslip Cleaning

Coverslips are cleaned by sonicating the coverslips twice for 30 minutes; once submerged in ethanol to remove organic material, and once in acetone to remove inorganic material. The coverslips are then washed with dH2O twice and dried in a petri dish.

For sonication, either one coverslip can be put into a 50 mL tube and submerged in the corresponding liquid, or a washing rack can be used, which can hold up to 10 coverslips. The washing rack was used from chapter 2.4 and onwards. The washing rack is more efficient in that fewer coverslips break, and the total number of coverslips that can be washed at the same time is higher.

2.2.2 PLL-PEG Coating

PLL-PEG is bound to the glass by making use of the positively charged PLL tail. The glass coverslips are negatively charged by using an oxygen plasma treater. The negatively charged side is named the working side. Directly after charging the glass, the coverslips are coated with PLL-PEG. Two methods for coating can be applied; the sandwich or the parafilm method.

The sandwich method uses pairs of coverslips, where the working sides are put onto each other with the volume of PLL-PEG in-between. The parafilm method puts the volume of PLL-PEG on a piece of clean parafilm, and puts the working side of the coverslip on top. The parafilm method creates a better monolayer of PLL-PEG, and disturbs the coating less during separation. Up to chapter 2.4.3 the sandwich method used. Chapter 2.4.4 and onwards uses the parafilm method.

For a 25 mm ø coverslip, 50 µL of PLL-PEG is used for both methods. The coverslips are then incubated for 30 minutes, separated, dried, and sterilized using UV for 30 minutes.

2.2.3 Micropatterning

Micropatterns are created in the PLL-PEG coating by using a photomask in the UV ozone cleaner. The photomask is made of quartz, and blocks the UV light except for the micropattern areas as shown in figure 3. The UV light that goes through removes the PLL-PEG for that area, creating micropatterns.

The coverslips are put working side up in the ozone cleaner. The photomask is cleaned with ethanol and put on top of the coverslips. The coverslips are then exposed to UV light for 5 minutes to create micropatterns.

2.2.4 ECM coating

To acquire cell adhesion in the micropatterns, an ECM coating is applied on the coverslip. The protein uses is vitronectin. A concentration of 5 µg/mL vitronectin is used with a volume of 50 µL using the sandwich method as described in chapter 2.2.2. The coverslips are incubated for 1 hour and separated. dPBS is added to the coverslips to prevent drying of the ECM coating.

2.2.5 Polyacrylamide Transfer

The micropatterns of PLL-PEG and ECM protein are now transferred onto PAA. This is done by polymerizing the acrylamide on this new coverslip with the micropatterned coverslip on top, and then separating the two coverslips, moving the micropatterns from the original coverslip to the now PAA coated coverslip. To make sure the PAA attaches to the new coverslip, the new coverslip is silanized prior to the polymerization process.

Silanization is done by marking and negatively charging one side of the coverslips as described in chapter 2.2.2 for the PLL-PEG coating. Then, a silanization mixture is made. This mixture of 1 mL contains 50 µL acetic acid, 6 µL of bind Silane Plus-One, and 950 µL of 95% ethanol. The parafilm method is used to coat a coverslip with 50 µL of silanization mixture. It is incubated for 1 hour, after it is washed with ethanol and dried.

The acrylamide solution for polymerization is made of 1 mL containing 125 µL 40% acrylamide, 50 µL 2% Bis solution, 50 µL HEPES 200 mM 8.5 pH and 775 µL dH2O. The solution is degassed in a centrifuge at maximum speed for 1 minute. 6 µL of APS and 4 µL of TEMED is added to start the polymerization process. The solution is vortexed, and using the sandwich method, 25 µL (for a 25 mm ø coverslip) of the acrylamide solution is used. The bottom coverslip is the silanized coverslip, while the top coverslip is the micropatterned coverslip. The coverslips are incubated for 20 minutes and separated gently using a scalpel. The silanized coverslip now contains the PAA gel, with the micropatterns on top, and will be used for cell seeding.

These coverslips can then be glued to the bottom in a regular 6 well plate, or on the bottom of a bottomless well plate using vacuum grease.

2.2.6 Cell Seeding

Before cell seeding, the coverslips are sterilized with UV light for 30 minutes. There are two types of used cardiomyocyte types in this research; human embryonal stem cell-derived ΔN3 Coup-red cardiomyocytes (hESC CMs) in culture, or Draggn-3A1-nkX 2.5 GFP-Actin-mRuby cardiomyocytes (Draggn CMs) from liquid nitrogen. The different types of cells were used due to the availability of the cell type.

The cardiomyocytes are either dissociated from the culture plate using TrypLE and MEF medium or thawed from liquid nitrogen. The cells are counted using a cell counting chamber and seeded at a cell density of around 400.000 cells per coverslip (~150.000 per cm^2). The used medium for further culture is CM GAL medium (cardiomyocyte medium with the addition of galactose). To this medium, several things are added; 0.3% T3, 0.01 % IGF, 1% Glucose, and 0.1% HCL 5 M. When using liquid nitrogen thawed cells, 1 in 100 RevitaCell is added to the medium. For a 6-well plate, 2 mL of medium is used per well. The experiment is then cultured in an incubator at 37°C.

Relevant results of cell attachment can be found between day 1 and day 7 after cell seeding using a brightfield microscope.

2.3 PLL-PEG & Vitronectin

This chapter describes the experiments using PLL-PEG only, or with the addition of vitronectin for ECM coating.

2.3.1 PLL-PEG Concentration & Passivation After UV Sterilization

3 different PLL-PEG concentrations were made; 0.1 mg/mL, 0.5 mg/mL, and 1 mg/mL. For each concentration of PLL-PEG, 2 clean coverslips were coated as described in chapter 2.2 and each glued in a well of a 6-well plate. No micropatterning or PAA transfer was applied. The coverslips were coated by covering them with 2 mL 5 µg/mL vitronectin and incubated for 1 hour. The vitronectin was them removed, and ~140.000 hESC CM cells were seeded per well after UV sterilization.

2.3.2 Micropatterns on Glass for PLL-PEG 0.5 mg/mL & 1 mg/mL

PLL-PEG 0.5 mg/mL and 1 mg/mL were made. For each concentration, 2 coverslips were coated, micropatterned, and covered with 2 mL 5 µg/mL vitronectin for 1 hour, and then UV sterilized and cell-seeded with 80.000 hESC CM cells per coverslip.

2.3.3 Vitronectin 5 µg/mL & 50 µg/mL

6 coverslips were coated with 0.5 mg/mL PLL-PEG and micropatterned. Vitronectin was prepared for both the concentration 5 and 50 µg/mL. For each concentration, 3 coverslips were coated. For the 5 µg/mL vitronectin, the coverslips were submerged in 2 mL 5 µg/mL vitronectin for 1 hour at room temperature. For 50 µg/mL vitronectin, the sandwich method is applied. The coverslips were PAA transferred and cell seeded with roughly 500.000 hESC CM cells per coverslip.

2.3.4 Effect of UV Sterilization after PAA transfer

6 coverslips were coated with 0.5 mg/mL PLL-PEG and micropatterned. They were coated with 50 µg/mL vitronectin and PAA transferred. Of the 6 coverslips, 3 were UV sterilized, and 3 were not UV sterilized. They were then cell seeded with ~450.000 cells per coverslip and put into a high-risk incubator.

2.4 PLL-PEG (FITC) & Gelatin

For these experiments, PLL-PEG and PLL-PEG FITC are used with gelatin as ECM coating.

2.4.1 PLL-PEG & Gelatin

6 coverslips with a diameter of 18 mm were coated with 0.5 mg/mL PLL-PEG and micropatterned. Gelatin was used as an ECM coating in 3 different methods.

2 coverslips were coated using the sandwich method using 13 µL 1% gelatin and incubated at room temperature for 1 hour, then washed with dH2O to get rid of excess gelatin by adding warm dH2O to cover the coverslip pair before separation.

2 coverslips were coated with 13 µL Gelatin and incubated on a hot plate at 40°C for 1 hour, then washed with warm dH2O. In a repeat experiment, this was repeated with both room temperature and warm water.

The coverslips were then PAA transferred using a volume of 13 µL acrylamide solution to obtain the same height (50 µm) of PAA gel. The coverslips were then glued to a bottomless well plate, UV sterilized, and cell seeded with 115.000 cells per coverslip.

2.4.2 PLL-PEG FITC & Gelatin

Six 18 mm ø coverslips were coated with 13 µL 1 mg/mL PLL-PEG FITC and micropatterned. They were ECM coated with 13 µL gelatin for 1 hour and washed with room temperature dH2O, PAA transferred, UV sterilized, and cell seeded with ~500.000 cells per coverslip.

The experiment was repeated with 2 PLL-PEG FITC coated coverslips with gelatin, and 2 PLL-PEG FITC coated coverslips with dH2O as a gelatin substitute. The volumes for PLL-PEG and gelatin are here standardized to 20 µL instead of 13 µL. These volumes are used in all following experiments. The coverslips are observed under a fluorescent microscope after PLL-PEG coating, micropatterning, ECM coating, PAA transfer, and after UV sterilization.

2.4.3 Excess PLL-PEG removal

6 clean coverslips were coated with 0.5 mg/mL PLL-PEG FITC. They were dried and washed twice with 1 mL HEPES 10 mM 7.4 pH. The coverslips were observed under a fluorescent microscope at all 3 stages. The coverslips were then micropatterned, gelatin-coated, PAA transferred, UV sterilized, and cell seeded with ~400.000 cells per coverslip.

This experiment was then repeated to check for consistency.

2.4.4 Effect of ozone cleaner times on micropatterns

12 coverslips were coated with 0.5 mg/mL PLL-PEG FITC and micropatterned for 0, 5, 10, 15, 20 or 30 minutes. They were then observed with a fluorescent microscope.

2.5 PLL-PEG FITC & Gelatin FITC

These experiments used the addition of gelatin FITC to PLL-PEG FITC. The gelatin FITC was made by mixing gelatin FITC 0.1% w/v with gelatin 10% w/v to obtain gelatin FITC 1% w/v.

2.5.1 Effect of gelatin FITC and UV activated areas

The PLL-PEG coating step was skipped. Instead, 2 coverslips were micropatterned, gelatin FITC coated, and observed using a fluorescent microscope. They were then PAA transferred, UV sterilized and cell seeded with ~400.000 hESC CM cells.

2.5.2 PLL-PEG FITC & Gelatin FITC Tracking and Cell Adhesion

2 coverslips were coated with 0.5 mg/mL PLL-PEG, washed with HEPES 10 mM 7.4 pH twice, micropatterning them, and coating them with gelatin FITC, transferring the micropatterns to PAA, UV sterilizing and cell seeding the coverslips at ~400.000 hESC CM cells per coverslip. The coverslips were observed with a fluorescent microscope after the gelatin FITC coating, and for both the coverslips after the PAA transfer.

Two other coverslips were coated with 0.5 mg/mL PLL-PEG FITC, washed with HEPES 10 mM 7.4 pH twice, micropatterned, gelatin-coated, and directly UV sterilized and cell seeded at ~400.000 hESC CM cells per coverslip. This experiment was observed after the gelatin coating to observe the micropattern quality.

The experiment was repeated to check for consistency.

2.6 PAA-gelMA 1% VS 5%

Instead of an ECM coating, gelMA was put into PAA for cell adhesion. This is done by replacing the dH2O of the acrylamide solution with gelMA.

2.6.1 PLL-PEG FITC & Regular PLL-PEG

2 coverslips were coated with 0.5 mg/mL PLL-PEG, and 2 coverslips with 0.5 mg/mL PLL-PEG FITC, washed twice with HEPES and micropatterned. For both PLL-PEG and PLL-PEG FITC coated coverslip, one of each was transferred onto either PAA containing 1% gelMA w/v or PAA containing 5% gelMA w/v. The coverslips were UV sterilized and cell seeded at ~400.000 hESC CM cells per coverslip.

2.6.2 PLL-PEG 0.5 mg/mL

4 coverslips were coated with 0.5 mg/mL PLL-PEG, washed twice with HEPES, and micropatterned. 2 of the coverslips were then transferred onto PAA containing 1% gelMA w/v, and 2 coverslips onto PAA containing 5% gelMA w/v. The coverslips were UV sterilized and cell seeded at ~400.000 hESC CM cells per coverslip.

2.6.3 PLL-PEG 1 mg/mL

4 coverslips were coated with 1 mg/mL PLL-PEG, washed twice with HEPES, and micropatterned. 2 of the coverslips were then transferred onto PAA containing 1% gelMA w/v, and 2 coverslips onto PAA containing 5% gelMA w/v. The coverslips were UV sterilized and cell seeded at ~400.000 hESC CM cells per coverslip. This experiment was then repeated to check for consistency.

2.6.4 Removal of electrostatic binding of PLL-PEG

4 clean coverslips were, without plasma treating, coated with 0.5 mg/mL PLL-PEG FITC. They were not washed, and micropatterned before directly transferring them onto PAA containing gelMA. 2 coverslips were transferred onto 1% gelMA in PAA, and 2 coverslips onto 5% gelMA in PAA. The coverslips were then UV sterilized and cell seeded with ~400.000 hESC cells per coverslip. This experiment was then repeated to check for consistency.

2.7 ECM Micropatterns

Here, the PLL-PEG coating is replaced with a coating of ECM. The ECM coating after micropatterning is removed. Different ECM proteins are experimented with.

2.7.1 ECM Protein Micropatterns – Gelatin FITC vs Fibronectin Alexa546

Using the parafilm method, 2 coverslips were coated with 20 µL 1% w/v gelatin FITC, and 2 with 20 ul 100 µg/mL fibronectin alexa546. They were incubated for 1 hour, micropatterned, transferred to PAA, UV sterilized, and cell seeded with 1 million hESC cells per coverslip.

2.7.2 ECM Protein Micropatterns – Vitronectin vs Fibronectin

2 clean coverslips were coated with 20 µL 50 µg/mL vitronectin, and 2 coverslips with 20 µL 50 µg/mL fibronectin. They were micropatterned, PAA transferred, UV sterilized and cell seeded at ~600.000 Draggn CM cells per coverslip.

The experiment was repeated similarly twice; once with 1.5 M cell seeding per coverslip, and once with 750.000 cells per coverslip.

3 Results

In this chapter, the results of the experiments as described in chapter 2 are shown. The experiments were done to see whether clear micropatterns can consistently be made on PAA with the use of PLL-PEG and ECM proteins. Different methods were used to test the effect of specific materials, concentrations or combinations on micropattern quality and consistency. Micropattern quality is defined by how well the micropattern parts and wafers of the photomask, as shown in figure 3, are translated to cell adhesion. The micropattern parts should have recognizable and complete shapes, whereas the wafer itself should be complete. Additionally, no cell attachment should be found outside of the micropattern parts, or the wafer.

The results come down to two types: brightfield images of the cell seeding with a 2x and 10x objective, which are used to show cell adhesion and micropatterns, and the fluorescent images of PLL-PEG FITC and fluorescent ECM proteins which are used to track the PLL-PEG and ECM proteins at several stages of the protocol.

3.1 PLL-PEG & Vitronectin

The original protocol uses PLL-PEG and vitronectin as micropattern materials. Here we use the same materials to recreate the results obtained by Vignaud et al.

3.1.1 PLL-PEG concentration & passivation after UV sterilization

In previous experiments by another researcher, unexpected cell attachment to PLL-PEG coated with vitronectin was found. This experiment was done to see whether the first UV sterilization step after the PLL-PEG coating affects the surface passivation of the PLL-PEG, or whether the PLL-PEG concentration affects the cell attachment. This experiment was done without PAA transfer. The results of the cell attachment on non-UV sterilized PLL-PEG can be found in figure 5.

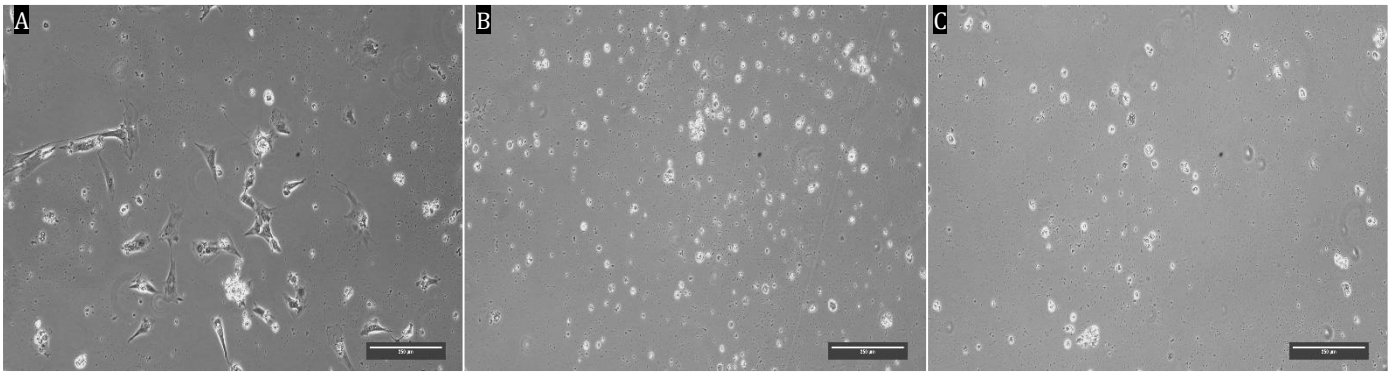

***Figure 5**: A shows the cell adhesion on a 0.1 mg/mL PLL-PEG coating, B for the 0.5 mg/mL PLL-PEG coating, and C for the 1 mg/mL PLL-PEG coating. Scalebars indicate 250 µm.*

In figure 5A, cell attachment can be seen for the concentration of 0.1 mg/mL PLL-PEG. For the higher concentrations of 0.5 and 1 mg/mL, no cell attachment can be found.

This shows that PLL-PEG on glass at concentrations higher than 0.5 mg/mL creates a sufficient anti-fouling coating. Therefore the next step of the protocol can be taken; creating micropatterns.

3.1.2 Micropatterns on glass for PLL-PEG 0.5 mg/mL & 1 mg/mL

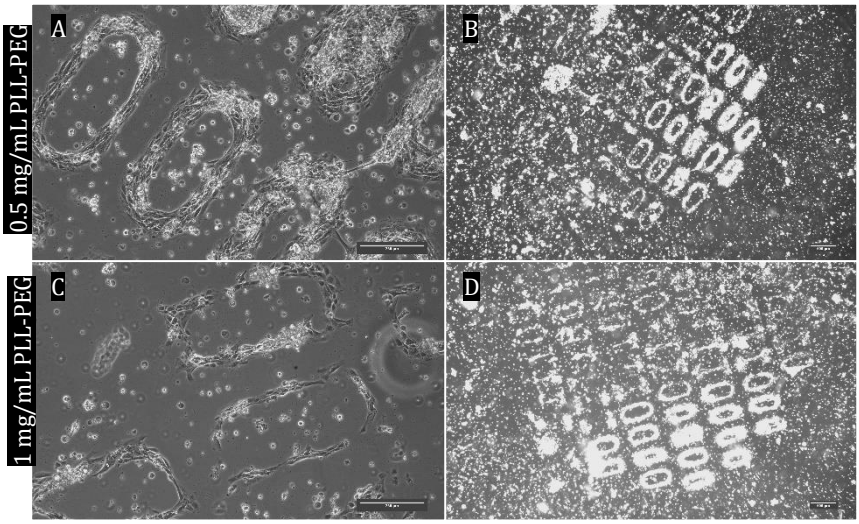

***Figure 6**: Shown is the micropatterns created on glass with 5 µg/mL vitronectin on either; A-B 0.5 mg/mL PLL-PEG or; C-D 1 mg/mL PLL-PEG. Scalebars A&C = 250 µm, B&D = 450 µm.*

Previously, PLL-PEG on glass was found to show sufficient anti-fouling properties. The addition of micropatterns and an ECM protein for cell adhesion can now be applied.

The effect on the surface passivation by micropatterning using the ozone cleaner was tested on both 0.5 mg/mL and 1 mg/mL PLL-PEG, with 5 µg/mL vitronectin as the ECM protein. This experiment was done without PAA transfer. The results of the cell adhesion on the created micropatterns on glass can be seen in figure 6.

The concentration of 0.5 mg/mL PLL-PEG shows clear, recognizable micro-patterns, although the patterns do not show the complete wafer. The 1 mg/mL PLL-PEG show clear micropatterns as well, also with incomplete wafers. In patterns show to be thinner than for the 0.5 mg/mL PLL-PEG. This shows that 0.5 mg/mL PLL-PEG gives better results, and that clear micropattern parts can be achieved on glass. The next step is to create the micropatterns on PAA, and try to find the optimal concentration of vitronectin.

3.1.3 Vitronectin 5 µg/mL & 50 µg/mL

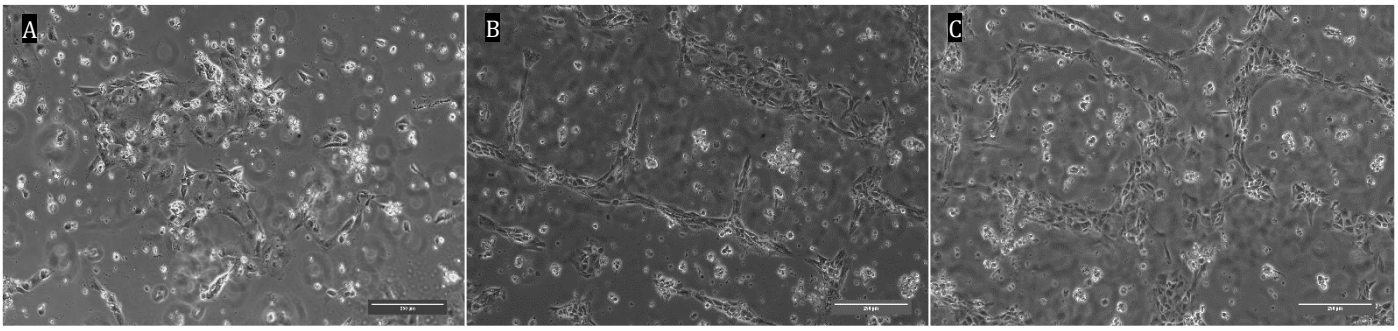

***Figure 7**: The effect of vitronectin micropatterns for A; 5 µg/mL vitronectin and B-C; 50 µg/mL vitronectin. Scalebar = 250 µm.*

To find the optimal concentration of vitronectin, two different concentrations were used; 5 and 50 µg/mL. Additionally, the micropatterns were transferred to PAA.

In two separate experiments, 5 µg/mL and 50 µg/mL vitronectin coatings were tested on PAA transferred micropatterns using 0.5 mg/mL PLL-PEG. As shown in figure 7, for 5 µg/mL vitronectin no micropatterns are found, but a lot of random attachment can be seen. For 50 µg/mL vitronectin clear patterns can be found, however, the cells have not grown in the micropatterns, which should contain vitronectin and no PLL-PEG, but on the sides and outside of the micropatterns, which should have only PLL-PEG. These type of micropatterns will be called ´inverse micropatterns´. The micropatterns also do not form complete wafer, only showing parts of the wafer.

This shows that the concentration of 50 µg/mL gives clearer patterns than 5 µg/mL. The only micropatterns that are created are, however, inversed. To see whether the UV sterilization has an effect on the vitronectin coating, the following experiment was done.

3.1.4 Effect of UV sterilization after PAA transfer

The UV sterilization step before the cell seeding could have an effect on the vitronectin coating, affecting cell adhesion and the micropattern quality. 0.5 mg/mL PLL-PEG was used, with 50 µg/mL vitronectin. As shown in figure 8 for both non-UV sterilized and UV sterilized coverslips, no cell adhesion and thus no micropatterns were observed.

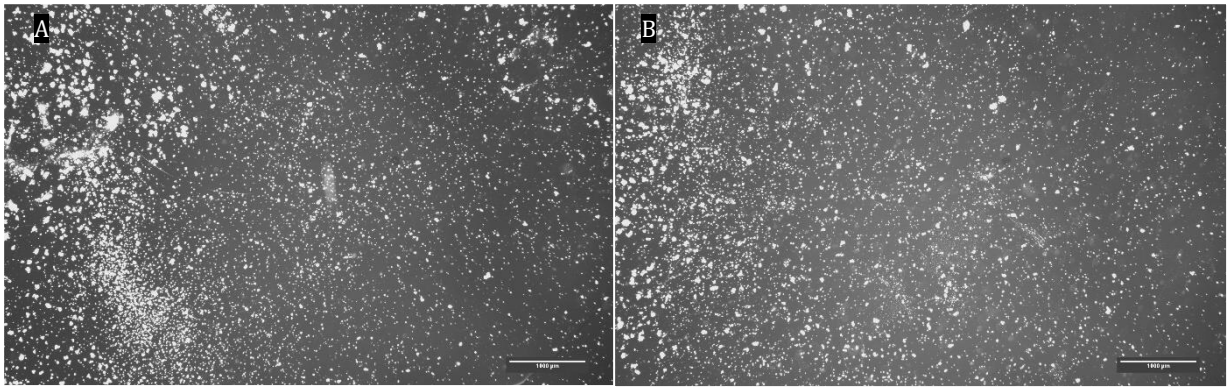

***Figure 8**: hESC CM cells seeded on 0.5 mg/mL PLL-PEG micropatterns with 50 µg/mL vitronectin on PAA hydrogel either A; non-UV sterilized or B; UV sterilized coverslips. Scalebar = 1000 µm.*

Instead of repeating the experiment, a substitute for vitronectin was used to see whether a cheaper alternative could be used to create correct micropatterns on PAA in the following experiment.

3.2 PLL-PEG (FITC) & Gelatin

As a substitute for vitronectin, gelatin was applied. Gelatin is a cheaper alternative ECM protein to vitronectin, with similar cell adhesive properties. Gelatin solidifies at room temperature, so several methods for gelatin coating were applied to see which method is optimal.

3.2.1 PLL-PEG & Gelatin

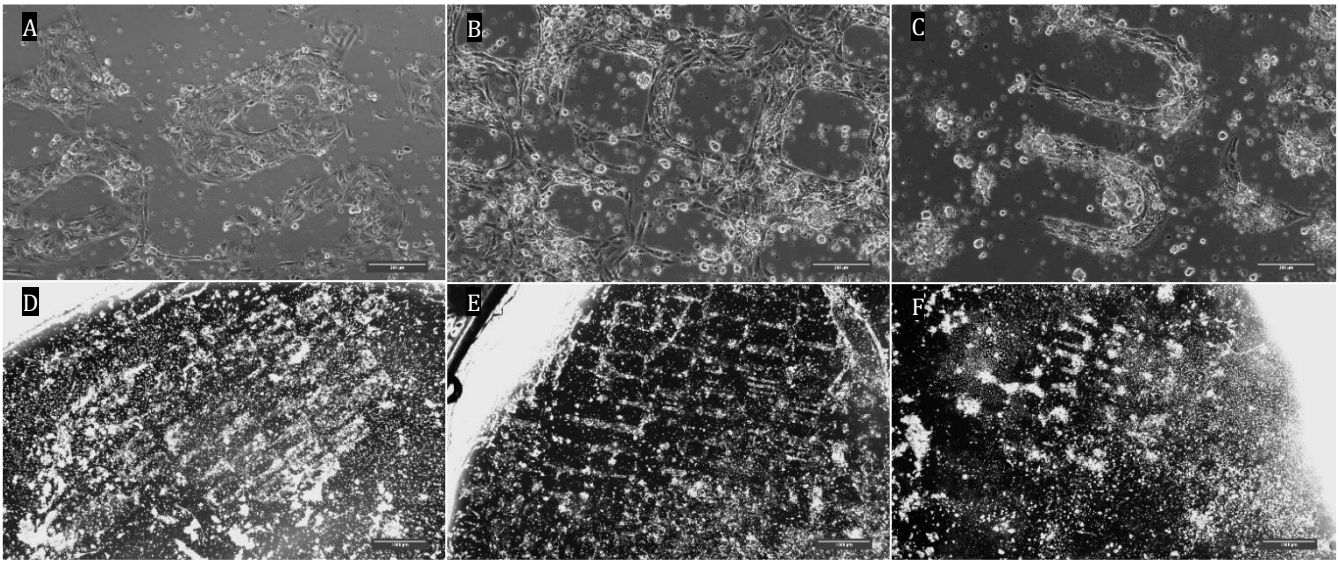

Figure 9: *Effect on cell adhesion of different methods of gelatin coating. Gelatin coating methods of A&D; incubated at room temperature and washed, B&E; incubated at 40°C and washed, and C&F; incubated at 40°C without washing. Scalebars A-C = 200 µm, D-F = 1000 µm.*

In the first experiment, three different methods of gelatin coating the micropatterns were tested; incubated at room temperature with washing, at 40°C with washing, and at 40°C without washing. The results are shown in figure 9, in which we can see that for all conditions, micropatterns are observed. For the room temperature incubated gelatin in figure 9A-C, near-complete wafers are shown, along with recognisable micropattern parts. For the 40 °C incubation with washing in figure 9B-E, inverse micropatterns are found, with cells adhering to the areas in between the micropattern parts instead of the inside of the micropatterns. The 40 °C without washing in figure 9C-F, incomplete micropattern wafers are found, where the parts of the micropatterns are also incomplete but recognisable.

However, for the repeats of the experiment, using incubation at room temperature or 40 °C temperature and washing with room temperature or 40 °C dH2O, no cell adhesion or micropatterns were observed.

Inconsistent results of micropatterns were obtained in these experiments; correct, inverse, and no micropatterns. This odd conformation of micropatterns may be due to wrong placement of PLL-PEG. Therefore, PLL-PEG FITC was obtained and will be used to observe what happens to the PLL-PEG coating.

3.2.2 PLL-PEG FITC & Gelatin

To track what happens to the PLL-PEG coating at all the steps of the protocol, PLL-PEG FITC was used. Fluorescent images were taken at each step of the protocol after the PLL-PEG coating, as shown in figure 10. The initial PLL-PEG coating shows to not have a monolayer, but rather a coating of droplets and larger areas of PLL-PEG covering the coverslip. The micropatterns created in this layer of PLL-PEG are clearly shown in figure 10B. The contrast between the UV irradiated areas and non-irradiated areas can be clearly observed. Droplets of intense PLL-PEG are still found all over the coverslip, in and outside the micropatterns.

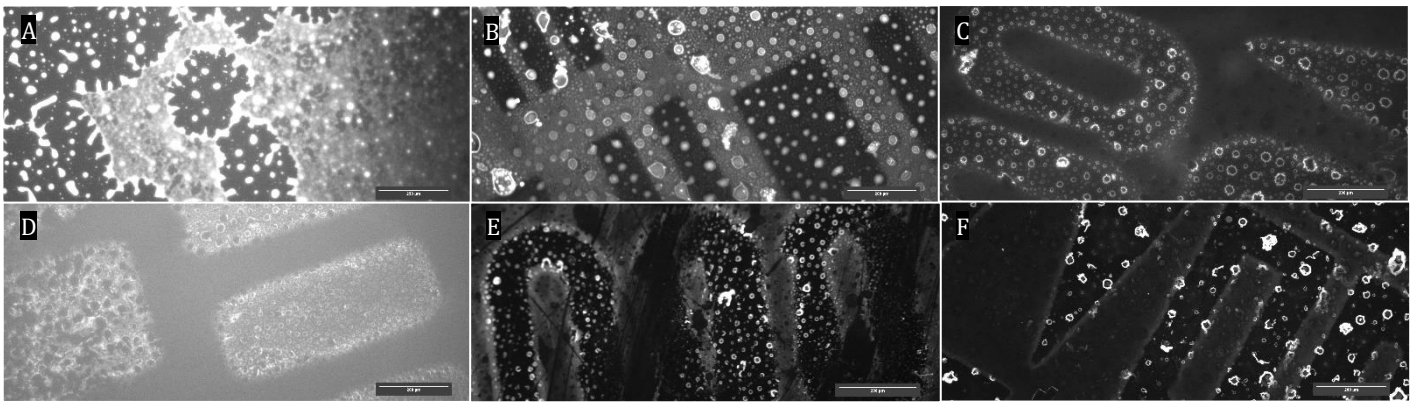

Figure 10: *fluorescent images of PLL-PEG FITC through all the steps of the protocol. A; after the PLL-PEG FITC coating. B; After micropatterning. C; after gelatin coating. D; the 18 mm ø coverslip on which the micropatterns were created after PAA transfer. E: the 25 mm ø coverslip on which the PAA hydrogel is polymerized and the micropatterns are transferred. F: the 25 mm ø coverslip after UV sterilization. Scalebar = 200 µm.*

After the gelatin coating, shown in figure 10C, micropatterns can still be clearly seen on the coverslip. However, an intense signal of PLL-PEG FITC droplet formation can now be observed only in the micropattern areas. After PAA transfer, which can be seen in figure 10D-E for the both used coverslips, it can be observed not all PLL-PEG was transferred onto the PAA hydrogel. The intensity of the signal is slightly higher for the original coverslip than for the PAA hydrogel coverslip. For the original coverslip in figure 10D, the intensity of PLL-PEG FITC inside the micropatterns is also higher than its surroundings, against expectations. Both coverslips show the droplet formation of PLL-PEG in the micropatterns. The UV sterilization step shows similar fluorescent signal compared to before the sterilization.

In the days following after cell seeding, no CM micropatterns were observed.

The experiment was repeated using either gelatin or water at the ECM coating step. The fluorescent images can be found in figure 11. Observed is that, even though the same protocol is used for PLL-PEG coating, a monolayer of PLL-PEG is created without droplet formation for all steps. The only significant difference between the gelatin and dH2O coating is that for gelatin, after the PAA transfer on the 25 mm ø coverslip, there is PLL-PEG in parts of the micropatterns with a higher intensity than its surroundings.

Cell seeding the coverslips resulted in no CM micropatterns for either condition.

Figure 11: *Fluorescent images of PLL-PEG coated with gelatin (A-C) or dH2O (D-F). A&D show the PLL-PEG FITC after coating. B&E show the PLL-PEG FITC for the 25 mm ø coverslip after PAA transfer. C&F show the PLL-PEG FITC for the 25 ø coverslip after PAA transfer. Scalebar = 200 µm.*

Both experiments resulted in no cell micropatterns. However, for these experiments it was also observed that after micropatterning and applying a liquid such as an ECM coating, PLL-PEG is observed inside the micropatterns. This may be the cause of the lack of cell attachment. To prevent PLL-PEG from moving

into the micropatterns, excess PLL-PEG can be washed away after coating, leaving only the bound PLL-PEG on the coverslip.

3.2.3 Excess PLL-PEG removal

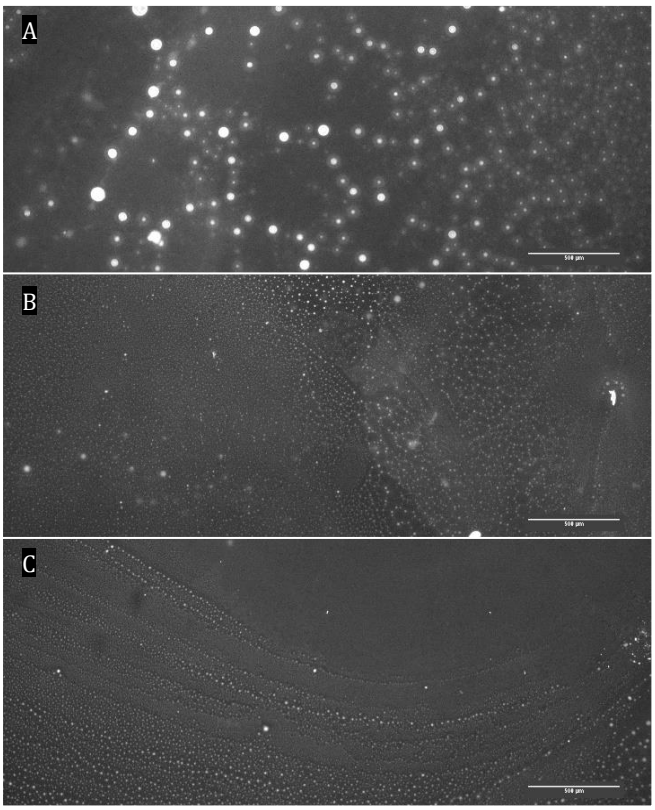

Figure 12: *PLL-PEG coating after A; 0 washes, B; 1 wash, and C; 2 washes with HEPES 10 mM 7.4 pH. Scalebar = 500 µm.*

Fluorescent signal is seen inside the micropatterns after ECM or dH2O coating. The liquid state of the ECM coating could enable excess PLL-PEG to move, and as the micropatterns are negatively charged after the ozone cleaner, the PLL-PEG could bind to these sites.

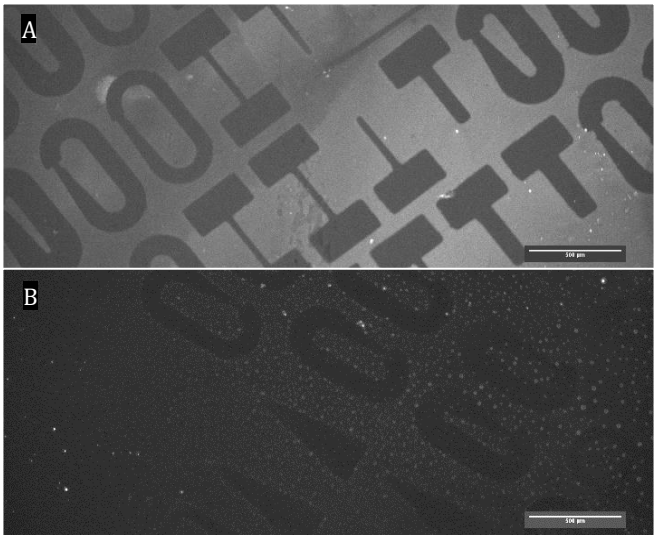

Figure 13: *PLL-PEG FITC on 25 ø coverslip after PAA transfer for experiment n=1 (A) and n=2 (B). Scalebar = 500 µm.*

To see whether excess PLL-PEG moves into the micropatterns during ECM coating, the PLL-PEG was washed after the PLL-PEG coating. This experiment was done twice (n=2).

Figure 12 shows the fluorescent images of the PLL-PEG coating at 0 washes, 1 wash or 2 washes with HEPES. For the 0 washes, we again see the droplets of PLL-PEG. For the 1st and 2nd wash, these droplets are smaller and significantly less present. The 2nd wash shows a more uniform coating of PLL-PEG than the 1st wash. Results for the repeat experiments were similar.

In figure 13, the final PLL-PEG coating after PAA transfer for both experiments is shown, while figure 14 shows the cell micropatterns for both experiments.

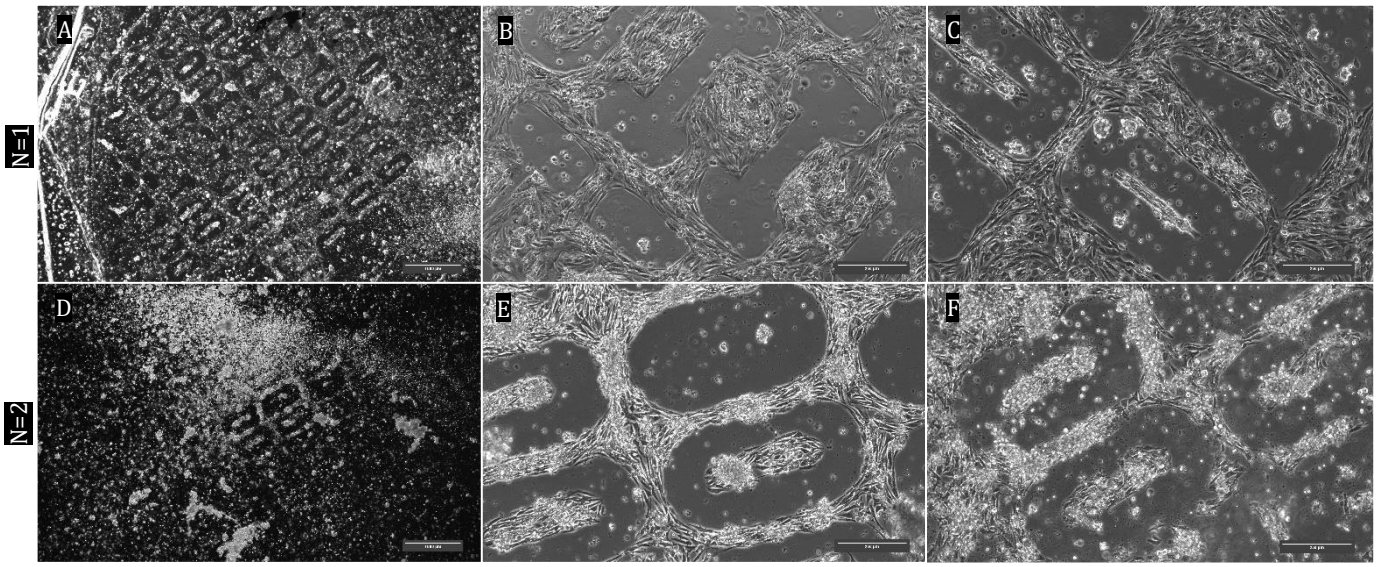

Figure 14: *Cell micropatterns on washed PLL-PEG with gelatin ECM coating for experiment n=1 (A-C) and experiment n=2 (D-F). Scalebar A&D = 1000 µm, BCEF = 250 µm.*

The PLL-PEG coating on the 25 mm ø coverslip shows clear micropatterns, with no droplet formation or higher intensity inside the micropatterns. The cell micropatterns found are, for both experiments, very clear and defined. Full wafers are found on the coverslips. However, again, the cells grow only on the outside of the micropattern areas, instead of inside, creating inverse micropatterns.

Washing the PLL-PEG after coating shows that no more PLL-PEG is found in the micropatterns after micropatterning and ECM coating. This results in clear micropatterns and complete, even though they are inverse. To observe whether the ECM coating is responsible for these inverse micropatterns, gelatin FITC can be used to track where the ECM protein is situated throughout the protocol.

3.2.4 Effect of ozone cleaner times on micropatterns

To see whether increasing times of using the ozone cleaner creates clearer and sharper micropatterns, 12 coverslips were coated with 0.5 mg/mL PLL-PEG FITC and micropatterned for 0, 5, 10, 15, 20 or 30 minutes. They were then observed with a fluorescent microscope. The images of the fluorescent micropatterns can be found in figure 15.

With an increase in time for UV radiation to create micropatterns, the fluorescent images do not show an increase in the quality of the patterns. The resolution and contrast of the patterns compared to the surroundings do not significantly improve.

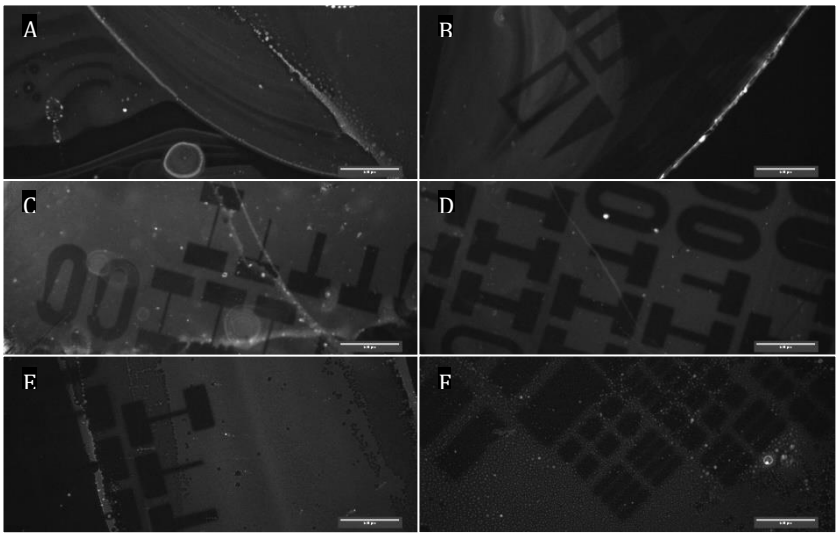

Figure 15: *Micropatterns at increasing UV irradiation times. A-F 0, 5, 10, 15, 20, 30 minutes respectively. Scalebar = 500 µm.*

Therefore the initial 5 minutes is kept as the standard time for micropatterning, as it shows to be the optimal time required.

3.3 PLL-PEG FITC & gelatin FITC

PLL-PEG FITC shows that the PLL-PEG ends up in the correct places, with the addition of washing after PLL-PEG coating. However, inverse micropatterns were still observed. Therefore, gelatin FITC is used as well to see whether the ECM coating is responsible for the inverse micropatterns on PAA.

3.3.1 Effect of gelatin FITC and UV activated areas

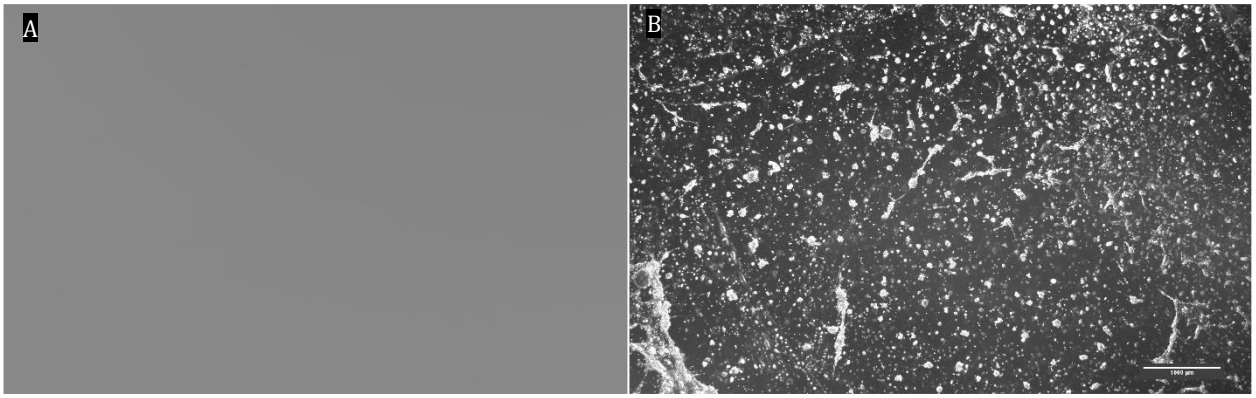

Figure 16: *A; The gelatin FITC coating and B; Cell adhesion on gelatin using the protocol without a PLL-PEG coating. Scalebar = 1000 µm.*

To see the effect of gelatin FITC location after micropatterning alone, no PLL-PEG coating was used. Micropatterning creates negatively charged areas, after which the coverslips are gelatin-coated, and transferred to PAA. The gelatin FITC coating and cell adhesion are shown in figure 16. The gelatin coating, under a fluorescent microscope, shows a monolayer of gelatin FITC. The cell seeding on this gelatin monolayer shows random attachment with no patterns.

This shows that gelatin creates a monolayer on the coverslip, regardless of UV activated areas.

3.3.2 PLL-PEG FITC & Gelatin FITC Tracking and Cell Adhesion

PLL-PEG FITC and gelatin FITC are used in separate conditions to track their location, to see whether either PLL-PEG or gelatin cause the inverse micropatterns. Because both cannot be observed at the same time, PLL-PEG FITC was used with gelatin, and separately PLL-PEG was used with gelatin FITC.

PLL-PEG FITC and gelatin are also tested for cell adhesion prior to the PAA transfer to observe the cell micropatterns before PAA transfer.

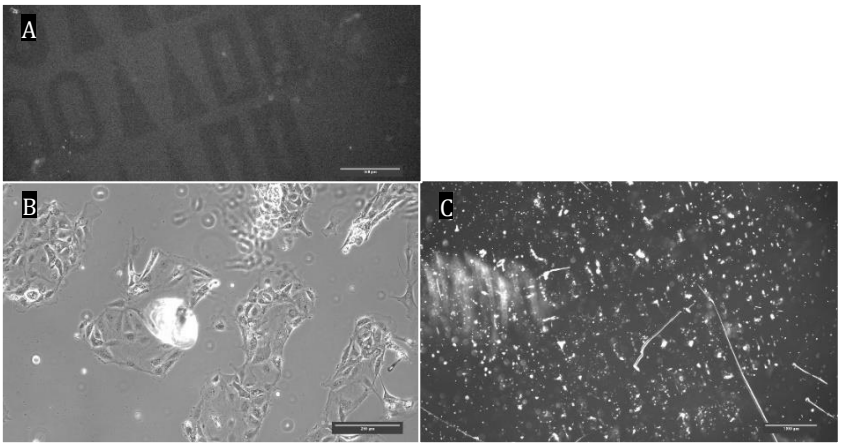

Figure 17*: PLL-PEG FITC and gelatin, without PAA transfer. A; the micropatterns after gelatin coating. B-C; the hESC CM cell adhesion. Scalebar A = 500 µm, B = 250 µm, C = 1000 µm.*

The results for PLL-PEG FITC and gelatin without PAA transfer can be seen in figure 17, which shows that there are clear micropatterns seen under the fluorescent microscope in figure 17A, a complete cell micropattern wafer is found in figure 17C, and the micropattern parts are recognisable as shown in figure 17B. The parts are not filled out completely with cardiomyocytes but show the distinct shapes.

The results for PLL-PEG and gelatin FITC can be observed in figure 18. Micropatterns of gelatin FITC can be seen in figures 18A-B, where A shows the gelatin FITC directly after gelatin coating, and B shows the gelatin FITC after PAA transfer on the 18 mm ø coverslip.

For both cases, the fluorescent signal of the gelatin is more intense inside the micropatterns. Directly after coating, the contrast of gelatin in and outside of the micropatterns is more intense than for the gelatin after PAA transfer. The micropatterns after PAA transfer are vague due to the lesser contrast, but still recognisable. The cell adhesion of figure 18C-D shows clear micropattern parts in an incomplete wafer. The parts of the micropattern show clear shapes, some more filled out than others.

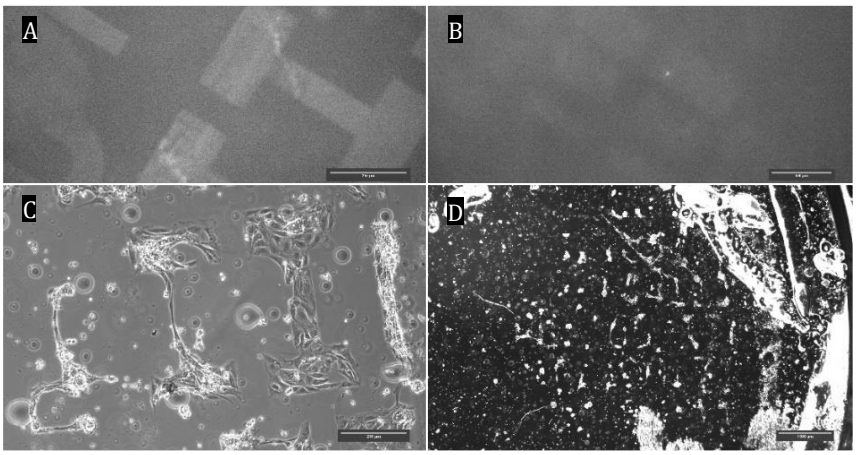

***Figure 18**: PLL-PEG with gelatin FITC. A; gelatin FITC after ECM coating. B; gelatin FITC after PAA onto 25 mm ø coverslip. C-D; cell adhesion on gelatin FITC micropatterns. Scalebar A&B = 500 µm, C = 250 µm, D = 1000 µm.*

For the repeated experiment, similar fluorescent results were found to figure 17 and 18. However, cell seeding gave no cell micropatterns for any condition.

Whereas the first experiment shows that correctly placed PLL-PEG and gelatin give cell micropatterns, the repeat experiment gave no micropatterns at all. To omit the ECM coating step and the possible complications this step brings to the micropatterns, the PAA can be made cell adhesive by the addition of gelMA. This may solve the inconsistency in micropattern results.

3.4 PLL-PEG & PAA-gelMA

To circumvent the use of the ECM coating, it was attempted to make the PAA gel cell adhesive. This way, the PLL-PEG micropatterns can be directly transferred onto PAA, making the PAA in the micropatterns cell adhesive, with the PLL-PEG surrounding it being non-cell adhesive. To do this, the dH2O in the acrylamide solution was replaced with gelMA of a final concentration in PAA of either 1% w/v or 5% w/v to check which concentration was optimal for cell adhesion.

3.4.1 PLL-PEG FITC & regular PLL-PEG

GelMA at a final concentration in PAA of 1 or 5 % w/v was tested as a replacement for the ECM coating. This was also compared using PLL-PEG FITC and regular PLL-PEG.

Figure 19 shows the results for cell adhesion on 1 and 5% gelMA in PAA with PLL-PEG FITC micropatterns. In figure 19A, the micropatterns show to be correct and distinct. However, while there is random cell attachment, no cell micropatterns can be found on the PAA-gelMA.

The cell adhesion on PLL-PEG micropatterns on PAA with 1 and 5% gelMA is shown in figure 20. For 1% gelMA, random cell attachment was found, but no cell micropatterns, as shown in figure 20A. For 5% gelMA in PAA, cell micropatterns were found. The wafers for these patterns are nearly complete, and the micropattern parts were recognisable. Some parts had cells that overlap with other parts. Random cell attachment was found on this PAA-gelMA concentration as well.

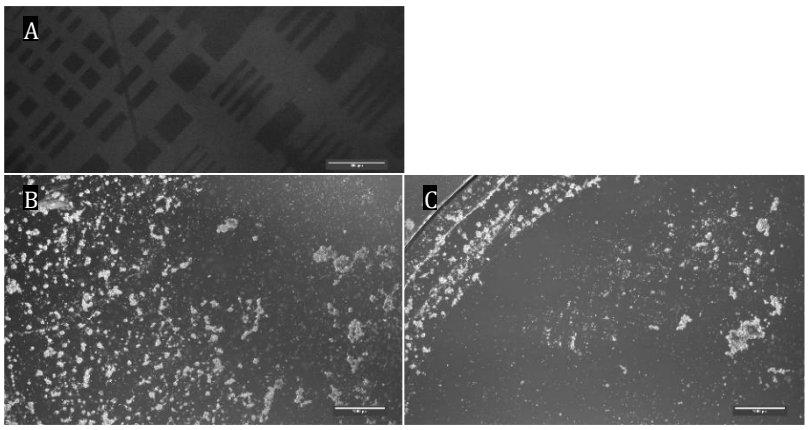

Figure 19: *PLL-PEG FITC micropatterns on PAA-gelMA. A; fluorescent image of PLL-PEG after PAA transfer onto the 25 mm ø coverslip. B; cell adhesion on 1% gelMA in PAA. C; cell adhesion on 5% gelMA in PAA. Scalebar A = 500 µm, B&C = 1000 µm.*

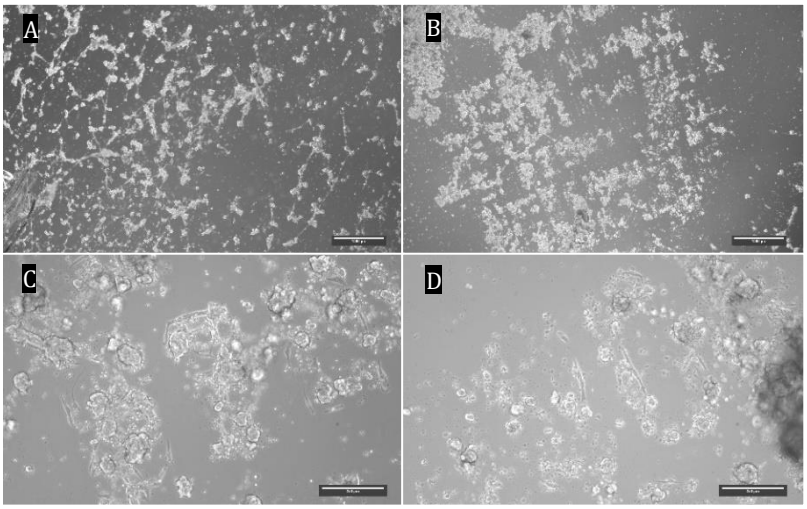

Figure 20: *PLL-PEG micropatterns on PAA-gelMA. A: cell attachment on 1% gelMA in PAA. B-D: cell attachment on 5% gelMA in PAA. Scalebar A&B = 1000 µm, C&D = 250 µm.*

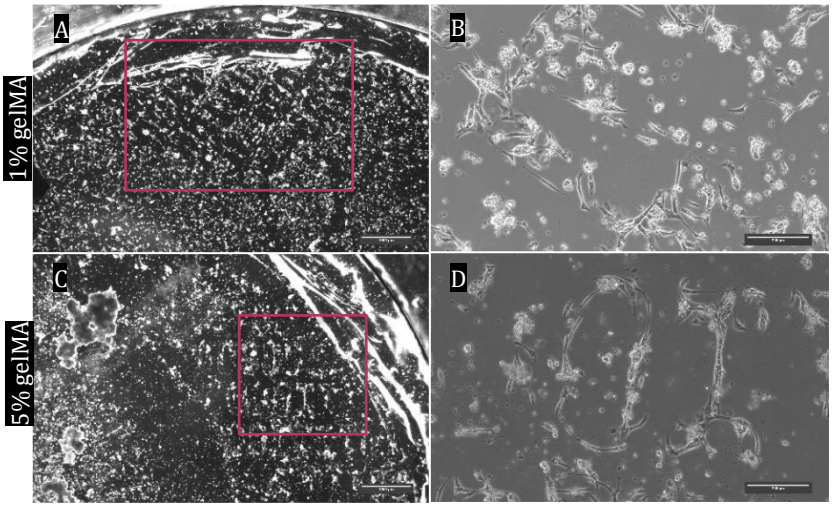

Figure 21: *cell adhesion on PLL-PEG micropatterns on PAA with A; 1% gelMA or B; 5% gelMA. Scalebar A&C = 1000 µm, B&D = 250 µm.*

With the use of PAA-gelMA instead of an ECM coating, we see that micropatterns can be achieved, if not consistently. However, in both cases, random cell attachment is found on the PAA-gelMA outside of micropattern areas. The PLL-PEG showed

micropatterns, and to see whether this can be reproduced, PLL-PEG at 0.5 mg/mL is again tried on PAA-gelMA in the next experiment.

3.4.2 PLL-PEG 0.5 mg/mL

The two different concentrations of gelMA are again tested for cell adhesion using only regular PLL-PEG 0.5 mg/mL.

Figure 21A-B show cell adhesion on PLL-PEG micropatterns with 1% gelMA in PAA. In figure 21A we can see there are some inversed micropattern parts, but in figure 21B no recognisable parts, inversed or not, can be distinguished. In figure 21C we see part of a micropattern wafer, and figure 21D shows there are micropattern parts that are recognisable shapes, however, they are not filled out completely. Again, for both gelMA concentrations, random attachment outside of the wafer locations is found.

Again micropatterns are found for PLL-PEG on PAA-gelMA. However, still random cell attachment is found outside of the micropattern areas. To see whether a better anti-fouling can be achieved, a higher concentration of PLL-PEG can be experimented with.

3.4.3 PLL-PEG 1 mg/mL

To try to increase the passivation effect of the PLL-PEG on gelMA, 1 mg/mL PLL-PEG was used for coating instead of 0.5 mg/mL PLL-PEG. From the results, as shown in figure 22 for both experiments 1 and 2 (n=2), it can be observed that for neither 1 or 5% gelMA in PAA there are cell micropatterns. There is still cell adhesion, though less than for 0.5 mg/mL PLL-PEG.

This shows that a higher concentration of PLL-PEG gives less cell adhesion, but also no micropatterns. The concentration of 0.5 mg/mL is preferable to this, as this results in micropatterns.

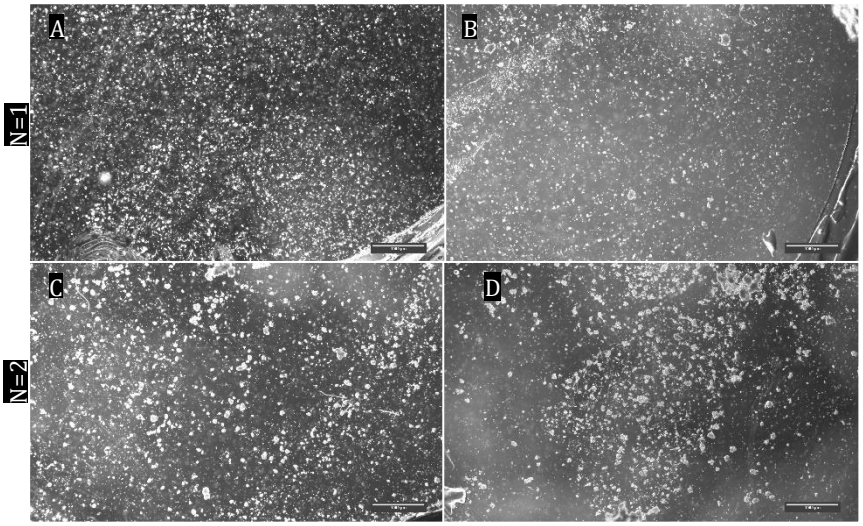

Figure 22: *cell adhesion for 1 mg/mL PLL-PEG with A&C; 1% gelMA in PAA and B&D; 5% gelMA in PAA. N stands for experiment 1 or 2. Scalebar = 1000 µm.*

3.4.4 Removal of electrostatic binding of PLL-PEG

In a meeting with Jacopo Movili, of Molecular Nanofabrication at the University of Twente, it was theorized that the electrostatic binding created between the negatively charged glass and the PLL-PEG is too strong, and therefore the PLL-PEG does not properly transfer onto the PAA. Now that PAA gelMA is used and no ECM coating is done, there is no liquid phase for the PLL-PEG to move before the PAA transfer. This makes it possible to not bind the PLL-PEG at all by removing the plasma treating step before PLL-PEG coating. To see whether this would improve the PLL-PEG transfer, and therefore the passivation and quality of the micropatterns, this was tested. The experiment was done twice.

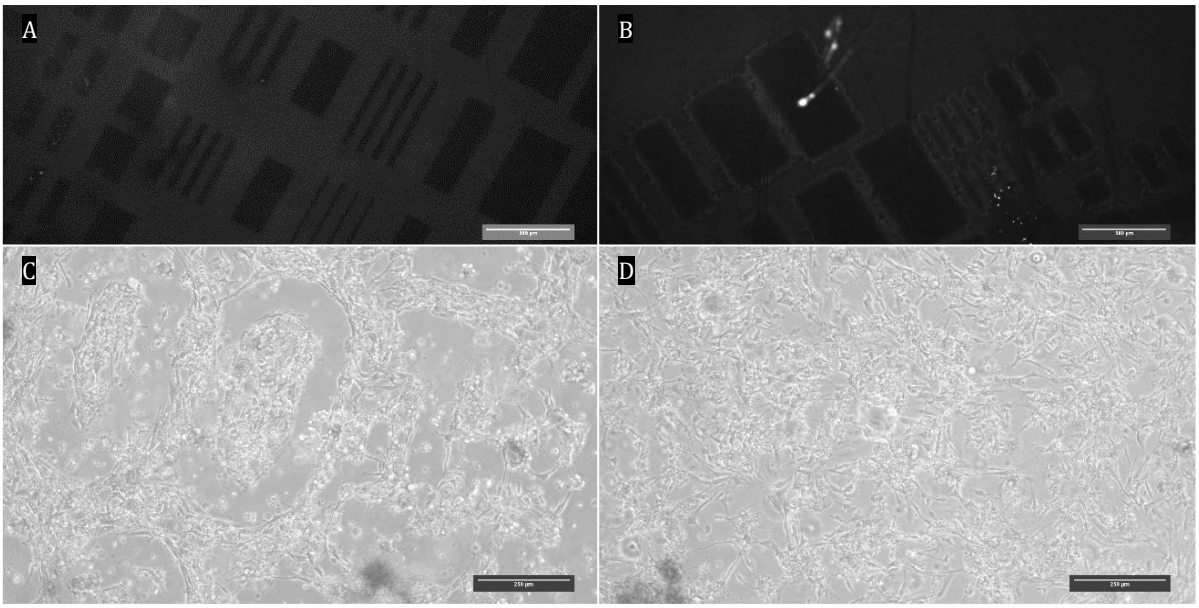

***Figure 23**: non plasma treated PLL-PEG on PAA-gelMA. A; experiment N=1, PLL-PEG FITC after PAA transfer onto 25 mm ø coverslip. B; experiment N=2, PLL-PEG FITC after PAA transfer onto 25 mm ø coverslip. C; cell micropatterns on 1% gelMA in PAA, N=2. D; cell adhesion on 5% gelMA in PAA, N=2. Scalebar A&B = 500 µm, C&D = 250 µm.*

For the first experiment, random cell attachment but no cell micropatterns were found for any conditions. The fluorescent image of PLL-PEG FITC after PAA transfer onto the 25 mm ø coverslip showed clear micropatterns for both experiments, as shown in figure 23A-B. For 1% gelMA in PAA, inversed cell micropatterns can clearly be observed in figure 23C, however for 5% gelMA in PAA in figure 23D only random cell attachment is found.

This shows that with unbound PLL-PEG on PAA-gelMA, either no or inverse cell micropatterns are created. This indicates that PLL-PEG itself may be responsible for the inverse micropatterns. Therefore if the use of PLL-PEG can be avoided entirely, consistent micropatterns may be achieved. This is tested in the following experiments by using only ECM proteins, and micropatterning those instead of the PLL-PEG before transferring them on PAA.

3.5 ECM micropatterns

To omit the use of PLL-PEG, it is theorized that micropatterns can be created in ECM proteins instead of PLL-PEG. To test this theory, different ECM proteins are tested for the creation of cell micropatterns on PAA after transfer. If done correctly, the cells should attach to the areas outside of the created micropatterns, as this is now coated with cell adhesive proteins.

3.5.1 ECM protein micropatterns – Gelatin FITC VS Fibronectin alexa546

This experiment uses the fluorescent ECM proteins gelatin FITC and fibronectin alexa546.

As shown in figure 24, gelatin shows no sign of contrast of the micropatterns as seen in PLL-PEG, indicating no micropatterns are created. This results in random cell attachment on the gelatin, as shown in figure 24C. For fibronectin, we see clear micropatterns in figure 24B, with cracks in between the micropatterns after the PAA transfer, indicating an incomplete transfer. Cell seeding on fibronectin micropatterns results in figure 24D, where cell attachment is found in the areas where fibronectin was seen in figure 24B, as was expected.

Fibronectin shows promise for the use of creating micropatterns with only ECM proteins on PAA. To see whether vitronectin behaves the same, or perhaps better than fibronectin, this is examined in the following experiment.

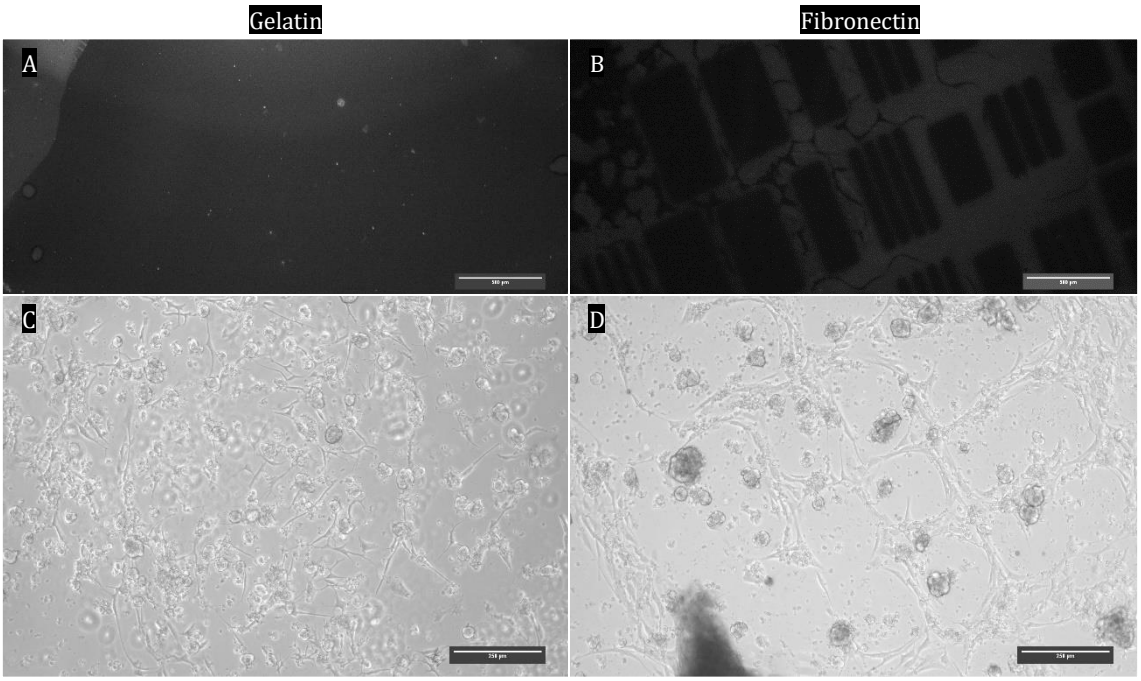

Figure 24: *gelatin FITC and fibronectin alexa546 micropatterns and subsequent cell seeding. A; gelatin after PAA transfer onto 25 mm ø coverslip. B; fibronectin after PAA transfer onto 25 mm ø coverslip. C; cell attachment on gelatin. D; cell attachment on fibronectin. Scalebar A&B = 500 µm, C&D = 250 µm.*

3.5.2 ECM protein micropatterns – Vitronectin vs Fibronectin

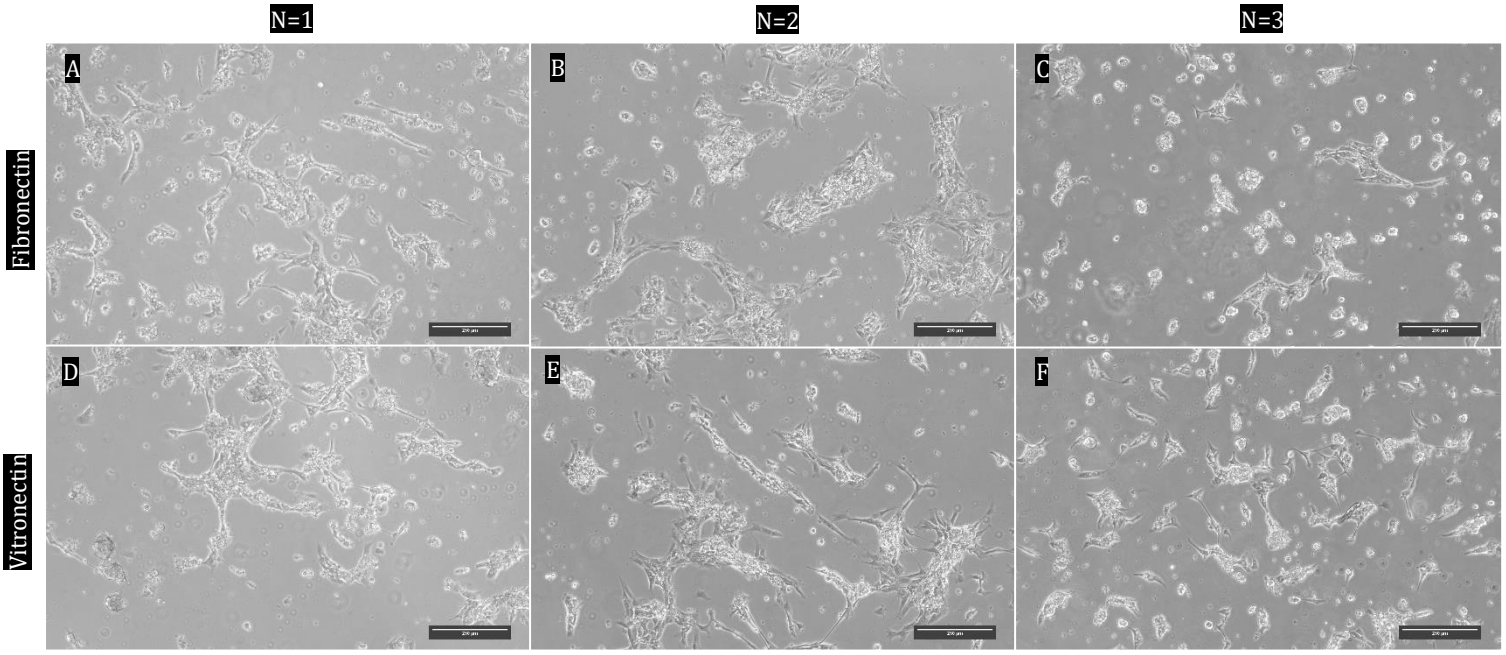

Figure 25: *Cell attachment on either fibronectin (A-C) or vitronectin (D-F), for experiments N=1 to 3. Scalebar = 250 µm.*

In addition to fibronectin, vitronectin was also tested for creating micropatterns. Cell seeding results are shown in figure 25, where figure A-C are cells seeded on fibronectin and D-F on vitronectin. The experiment was repeated thrice (N=3). For all experiments, it can be observed that no consistent clear cell micropatterns were created. For fibronectin in N=2, figure 25B, an inverse micropattern shape can be distinguished, this did not show in any of the other experiments. For vitronectin, only random cell attachment was found, with some fragments of what seem to be cells growing at perpendicular angles.

For both ECM proteins, micropatterns can be achieved, but they are not complete or consistent. However, it does show promise, and if optimized in future experiments may prove sufficient for the creation of micropatterns on PAA.

3.6 Result Summary

All the results obtained from the experiment are condensed in this chapter by the use of table 1, which marks what the results showed chronologically from top to bottom. Shown is on what substrate the cells were grown; glass, PAA, or PAA-gelMA. Then is shown whether any cell attachment was found, followed by whether micropattern parts were observed, whether the wafers of micropatterns were complete, if the micropatterns found were correct or inverted, and whether repeating experiments were consistent.

These results are marked and colour-coded in categories with a checkmark for positive, a cross for negative, or a dash for not applicable. See table 1 for the rundown of the results. When repeated experiments give inconsistent results, both a checkmark and a cross are used. The only experiments where complete micropattern wafers were found were for the experiments 'PLL-PEG FITC & gelatin FITC tracking and Cell Adhesion" and "PLL-PEG FITC & regular PLL-PEG". All other experiments showed either no micropatterns, incomplete wafers, or inverted micropatterns.

***Table 1**: Rundown of the results with checkmarks for positives, crosses for negatives, and dashes for not applicable.*

	Cell culture substrate	cell attachment	micropattern parts	Complete Micropattern wafers	Correct micropatterns	Consistent results in repeat experiments
	PLL-PEG & vitronectin					
PLL-PEG Concentration & Passivation after UV Sterilization	Glass	×	-	-	-	-
Micropatterns on Glass for PLL-PEG 0.5 mg/mL & 1 mg/mL	Glass	✓	✓	×	✓	-
Vitronectin 5 µg/mL & 50 µg/mL	PAA	✓	✓	×	×	-
Effect of UV sterilization after PAA transfer	PAA	×	-	-	-	-
	PLL-PEG (FITC) & Gelatin					
PLL-PEG & Gelatin	PAA	✓	✓	×	✓×	×
PLL-PEG FITC & Gelatin	PAA	✓	×	×	-	✓
Excess PLL-PEG removal	PAA	✓	✓	✓	×	✓
Effect of ozone cleaner times on micropatterns	-	-	-	-	-	-
	PLL-PEG FITC & Gelatin FITC					
Effect of gelatin FITC and UV activated areas	PAA	✓	×	×	-	-
PLL-PEG FITC & Gelatin FITC Tracking and Cell Adhesion	PAA	✓	✓×	✓×	✓	×
	PLL-PEG & PAA-gelMA					
PLL-PEG FITC & regular PLL-PEG	PAA-gelMA	✓	✓	✓	✓	-
PLL-PEG 0.5 mg/mL	PAA-gelMA	✓	✓	×	✓	-
PLL-PEG 1 mg/mL	PAA-gelMA	✓	×	×	-	✓
Removal of ionic binding of PLL-PEG	PAA-gelMA	✓	✓	×	×	×
	ECM micropatterns					
ECM protein micropatterns – Gelatin FITC vs Fibronectin alexa546	PAA	✓	✓	×	✓	-
ECM protein micropatterns – Vitronectin vs Fibronectin	PAA	✓	✓	×	✓	×

4 Discussion

The creation of inverse patterns, where regular patterns were the target result, is the largest point of discussion here. These inverse patterns were created several times, often where similar to equal protocols were applied. These patterns were also not only created when an ECM protein was used, but also with the use of only PLL-PEG on PAA-gelMA, while fluorescent images show the correct transfer of PLL-PEG and ECM proteins, but showing both correct and inverse cell micropatterns.

Several theories on why these inverse cell micropatterns occur are discussed here, each with their reasoning and substantiation.

Theory 1: Electrostatic attraction and layer thickness.

The first theory on the creation of inverse patterns is based on the electrostatic attraction created during PLL-PEG coating and UV micropatterning. PLL-PEG binds electrostatically to the glass after plasma treating, due to the then negative charge of the glass and positive PLL tail of the PLL-PEG at pH 7.4. The micropatterns created during UV irradiation are negatively charged. This is also why excess PLL-PEG moves into these spaces when a liquid phase is added. The charge of this area can also affect the binding of an ECM protein to the surface. As the surface is negatively charged, it interacts differently with these proteins depending on their isoelectric point and the pH. At neutral pH, vitronectin, fibronectin and gelatin type A are above their isoelectric point. This makes the proteins overall negatively charged, which would create an electrostatic repulsion effect. [63, 65, 85]

During plasma treatment, which occurs by using the plasma treater or ozone cleaning machine, two processes may occur with the use of glass. The first is the effect intended for this research; the removal of organic material. This effect creates the micropatterns. The second effect is the formation of polar carbon groups on the surface. This increases the hydrophilicity of the surface, thus increasing the wettability of the glass, and adhesion properties. [86]

It is possible that the adhesion of the PLL-PEG and ECM protein to the glass is too strong to properly transfer to the PAA hydrogel after polymerization. Instead what could happen is that during ECM coating, a complete coating of the ECM protein is done on both the micropattern areas on glass, and the PLL-PEG surrounding it. The ECM is bound to the glass strongly, while the ECM on top of the PEG is not bound due to the properties of PEG. During transfer, only the ECM on top of the PEG transfers properly, leaving the correct pattern of PLL-PEG and ECM behind. This would create inverse micropatterns.

Additionally, if the layer of ECM protein is too thin or does not coat the PLL-PEG and instead only binds to the glass, no ECM transfer to the PAA gel would occur, and no cell adhesion would be found. This would explain the experiments where PLL-PEG fluorescent images are found to be correct, even after transfer, but no cell adhesion is found. Depending on the binding strength, and the thickness of the layers of PLL-PEG or ECM coating, either correct, inverse, or no cell micropatterns would be created.

However, with the use of PLL-PEG, no ECM protein coating, and PAA-gelMA, where PLL-PEG is not electrostatically bound to the glass, inverse cell micropatterns are also found. This means that the cells attach to the PLL-PEG coated areas on PAA-gelMA, and not to the PAA-gelMA at all. The fluorescent images of PLL-PEG on the PAA-gelMA hydrogel show that there is a correct location and deposit of PLL-PEG. This brings us to theory 2.

Theory 2: Cell adhesive PLL-PEG

While poly(ethylene glycol) is an anti-fouling molecule, PLL has shown to be a cell adhesive molecule and has been extensively used as such in cell culture. [87, 88] PLL and PLL-PEG have also been used together to create cell adhesive and anti-fouling areas respectively. [89] The cell attachment to PLL-PEG on PAA-

gelMA is shown in the performed experiments, and only to the PLL-PEG coated areas. This can only mean that cells adhere to the PLL-PEG somehow, and even prefer it to PAA.

It could be that the cell adhering properties of PLL dominate the anti-fouling properties of the PEG. The conformation of the PLL-PEG molecule could be the key factor here. On glass, a carpet-like structure of PEG is created due to the PLL-glass binding, giving the correct anti-fouling properties as seen in the first experiment done. If this conformation of the molecule holds during and after transfer, the PEG top layer would be caught in the PAA polymerization. During transfer, the PLL-glass binding is separated, and this could create a top layer of PLL instead. This PLL could then perform its cell adhesive properties, creating inverse cell micropatterns. This fits with the fact that we do see fluorescently tagged PLL-PEG on the correct spaces, yet cell adhesion is found on PLL-PEG. However, this is not always the case. When fluorescently tagged PLL-PEG FITC was used, and on separate coverslips but in the same experiment gelatin FITC was used, both materials were found in the correct places; PLL-PEG surroundings, with gelatin in the micropatterns. This created correct micropatterns, with cells adhering only to the gelatin. This could again depend on the transfer of PLL-PEG, how the molecule conformation is after transfer. However, we also see inverse micropatterns when no electrostatic binding is applied to bind PLL-PEG to glass. This should result in random attached PLL-PEG, with no specific conformation. Still, cell attachment to PLL-PEG is observed. This brings us to the last theory.

Theory 3: Acrylamide polymerization affects PLL-PEG properties

If cells adhere to PLL-PEG, but only after acrylamide polymerization, perhaps one of the components used in the polymerization of acrylamide affects the PLL-PEG anti-fouling properties. These components include ammonium persulfate (APS), TEMED, acrylamide and bis-acrylamide, with the possible addition of gelMA. However, previous research with similar methods and materials, as done by Vignaud et al, do not encounter adhesive PLL-PEG.

To find out exactly how inverse cell micropatterns occur, more experiments and research should be done to confirm these theories whether PLL-PEG becomes cell adhering because of the transfer method, or the binding to glass of both ECM and PLL-PEG creates an inconsistent transfer of these materials. Simultaneous use of differently fluorescent-tagged PLL-PEG and ECM protein should be done, with several experiments to check for the inconsistencies found, and additional experiments for only PLL-PEG on PAA or PAA-gelMA.

Also notable for the experiments where no cell adhesion or cell micropatterns were found is that the cell used were not of the same quality per batch. The quality of the batch differed significantly and may be the cause of low cell adhesion. This, in addition to where micropatterns were created but were found to be filled with a low number of cells, overseeding of the experiment can be applied to assure maximum cell adhesion.

Many micropatterning techniques were designed over the year. Only a number of these micropatterning methods are serviceable for specifically creating micropatterns on hydrogel or a micropattern shaped hydrogel. And for creating micropatterns with specific cell adhering and cell repellant areas on a PAA hydrogel, allowing the monitoring of both fluorescent cells, and fluorescent beads in the PAA, even fewer methods can be applied. A monolayer of PAA underneath the micropatterns is required for this method, which means the micropatterns need to be created on top of the PAA, during or after polymerization. The micropatterns themselves cannot have a substantial thickness, as the contraction of the cells on PAA is measured, and a different material with a non-negligible thickness in between the cells and the substrate will affect this measurement significantly. Next to that, the micropattern requires the use of two proteins, instead of the conventional single protein micropatterns. Alternative methods which meet all these requirements are, up until now, few in numbers.

In 2014 Desai et al designed a stamp that is made by microcontact printing, and can carry distinct pattern with multiple proteins. The technique is named 'stamp-off', and instead of destroying the protein by UV or plasma exposure, it stamps specific areas of the protein monolayer onto a UV ozone treated template, removing undesired areas of protein from the stamp. Subsequent re-inking with proteins and stamp-off can be performed on differently patterned UV ozone treated templates. Fibronectin, vitronectin, and collagen have been used with this method. [90] This method creates a similar result to the micropatterns on glass designed in this research, with similar micropattern resolution. Whether this method would solve the issues found in this research is unclear, although it does show potential as an alternative of similar potential.

Another method uses a lithography technique to obtain multi-protein patterning, with the use of protecting pre-existing features through a design that achieves high precision alignment between substrate and mask. This high precision alignment creates the possibility to remove or coat specific areas in sequence. The precision achieved with this method is ~10 μm, which is similar to the precision of micropatterns achieved with the method used in this research. [90]

These methods show that there are alternative ways to create multi-protein micropatterns, which show similar potential to Vignaud et al's research. These alternative methods may prove to avoid the problems that were encountered by using Vignaud et al's methods, although the encountered issues with Vignaud et al's method may yet be resolved if more research is done, preparing the way for upscaling the creation of micropatterns for the research of cardiomyocyte function.

5 Conclusion

The purpose of this research was to optimize the protocol used to create consistent and recognizable micropatterns on polyacrylamide (PAA). This optimization is required before upscaling to a 96 well plate can be commenced. This upscaling would show great potential for the drug development industry. To endeavor optimization of the protocol, several additions and variants of the original protocol by Vignaud et al. have been made and tested. [7]

Regarding the creation of micropatterns, two different conclusions can be made. First, the most consistent and correct micropatterns were made using bound PLL-PEG at a concentration of 0.04 $\mu g/mm^2$, transferred to PAA containing 5% w/v gelMA. The micropatterns made of only ECM protein on PAA show promise for cell micropatterns as well, however fewer cell micropatterns were found compared to bound PLL-PEG on PAA-gelMA.

Secondly, the highest quality cell micropatterns were found for washed PLL-PEG with gelatin ECM on PAA. These micropatterns had the best translation of photomask to patterns, however these cell micropatterns were inversed, making them unusable for upscaling without further experimentation to figure out how the inverse patterns are created.

Additionally, the washing of PLL-PEG after coating with HEPES removes the excess of PLL-PEG. This is important to micropattern creation, as unbound PLL-PEG has shown to move into the surface activated areas after micropatterning after coming in contact with a liquid, such as the ECM coating step. The PLL-PEG in the micropattern areas counteracts the cell adhesive properties of the ECM coating. With the removal of this unbound PLL-PEG with washing, these counteractive properties are avoided, which significantly increases micropattern quality.

Other found optimizations or alternatives for the steps used in the original protocol are listed below.

- Not UV sterilizing the PLL-PEG after coating gives good anti-fouling qualities of PLL-PEG on glass.
- The optimal concentration of PLL-PEG for anti-fouling is 0.04 $\mu g/mm^2$.
- The optimal concentration of ECM proteins for cell adhesive properties is 0.004 $\mu g/mm^2$.
- The optimal volume for complete coverage of the coverslip is 7.9 $\mu L/cm^2$.
- A time of 5 minutes in the UV ozone cleaner for the creation of micropatterns is sufficient, additional time does not improve the patterns.
- An easy alternative to the ECM coating step is the addition of gelMA in the acrylamide solution. The gelMA at the desired concentration replaces the dH2O in the acrylamide solution.
- The PLL-PEG can be avoided completely by micropatterning an ECM protein coating directly. The PAA will act as an anti-fouling substrate, with ECM micropatterns on top. However, this needs to be optimized further to be used for consistent micropattern creation.

References

1. network, E.h. *European Cardiovascular Disease Statistics 2017*. Available from: http://www.ehnheart.org/cvd-statistics.html.
2. Tallawi, M., et al., *Effect of substrate mechanics on cardiomyocyte maturation and growth.* Tissue engineering. Part B, Reviews, 2015. **21**(1): p. 157-165.
3. Woodcock, E.A. and S.J. Matkovich, *Cardiomyocytes structure, function and associated pathologies.* Int J Biochem Cell Biol, 2005. **37**(9): p. 1746-51.
4. Rog-Zielinska, E.A., et al., *The Living Scar--Cardiac Fibroblasts and the Injured Heart.* Trends in molecular medicine, 2016. **22**(2): p. 99-114.
5. Beans, C., *Inner Workings: The race to patch the human heart.* Proceedings of the National Academy of Sciences of the United States of America, 2018. **115**(26): p. 6518-6520.
6. *Medication for the long-term treatment of coronary artery disease.*: Institute for Quality and Efficiency in Health Care (IQWiG).
7. Vignaud, T., H. Ennomani, and M. Thery, *Polyacrylamide hydrogel micropatterning.* Methods Cell Biol, 2014. **120**: p. 93-116.
8. Takeda, M., et al., *Development of In Vitro Drug-Induced Cardiotoxicity Assay by Using Three-Dimensional Cardiac Tissues Derived from Human Induced Pluripotent Stem Cells.* Tissue engineering. Part C, Methods, 2018. **24**(1): p. 56-67.
9. Bernstein, D., *Induced Pluripotent Stem Cell-Derived Cardiomyocytes: A Platform for Testing For Drug Cardiotoxicity.* Progress in pediatric cardiology, 2017. **46**: p. 2-6.
10. Cowger, J.A., *Addressing the Growing U.S. Donor Heart Shortage.* Waiting for Godot or a Transplant?, 2017. **69**(13): p. 1715-1717.
11. staff, M.c. *Stem cells: What they are and what they do*. Available from: https://www.mayoclinic.org/tests-procedures/bone-marrow-transplant/in-depth/stem-cells/art-20048117.
12. Vazin, T. and W.J. Freed, *Human embryonic stem cells: derivation, culture, and differentiation: a review.* Restorative neurology and neuroscience, 2010. **28**(4): p. 589-603.
13. Koivumäki, J.T., et al., *Structural Immaturity of Human iPSC-Derived Cardiomyocytes: In Silico Investigation of Effects on Function and Disease Modeling.* Frontiers in physiology, 2018. **9**: p. 80-80.
14. Machiraju, P. and S.C. Greenway, *Current methods for the maturation of induced pluripotent stem cell-derived cardiomyocytes.* World journal of stem cells, 2019. **11**(1): p. 33-43.
15. Jiang, Y., et al., *Maturation of Cardiomyocytes Derived from Human Pluripotent Stem Cells: Current Strategies and Limitations.* Molecules and cells, 2018. **41**(7): p. 613-621.
16. Scuderi, G.J. and J. Butcher, *Naturally Engineered Maturation of Cardiomyocytes.* Frontiers in Cell and Developmental Biology, 2017. **5**: p. 50.
17. Lundy, S.D., et al., *Structural and functional maturation of cardiomyocytes derived from human pluripotent stem cells.* Stem Cells Dev, 2013. **22**(14): p. 1991-2002.
18. Passier, R., V. Orlova, and C. Mummery, *Complex Tissue and Disease Modeling using hiPSCs.* Cell Stem Cell, 2016. **18**(3): p. 309-21.
19. Mannhardt, I., et al., *Human Engineered Heart Tissue: Analysis of Contractile Force.* Stem cell reports, 2016. **7**(1): p. 29-42.
20. Fermini, B., S.T. Coyne, and K.P. Coyne, *Clinical Trials in a Dish: A Perspective on the Coming Revolution in Drug Development.* SLAS discovery : advancing life sciences R & D, 2018. **23**(8): p. 765-776.
21. Besser, R.R., et al., *Engineered Microenvironments for Maturation of Stem Cell Derived Cardiac Myocytes.* Theranostics, 2018. **8**(1): p. 124-140.
22. Nguyen, N., et al., *Adult Human Primary Cardiomyocyte-Based Model for the Simultaneous Prediction of Drug-Induced Inotropic and Pro-arrhythmia Risk.* Frontiers in physiology, 2017. **8**: p. 1073-1073.
23. Hersch, N., et al., *The constant beat: cardiomyocytes adapt their forces by equal contraction upon environmental stiffening.* Biology open, 2013. **2**(3): p. 351-361.
24. Forte, G., et al., *Substrate stiffness modulates gene expression and phenotype in neonatal cardiomyocytes in vitro.* Tissue Eng Part A, 2012. **18**(17-18): p. 1837-48.
25. Syed, S., A. Karadaghy, and S. Zustiak, *Simple polyacrylamide-based multiwell stiffness assay for the study of stiffness-dependent cell responses.* Journal of visualized experiments : JoVE, 2015(97): p. 52643.
26. Ahola, A., et al., *Simultaneous Measurement of Contraction and Calcium Transients in Stem Cell Derived Cardiomyocytes.* Ann Biomed Eng, 2018. **46**(1): p. 148-158.
27. Sharma, A., et al., *Differentiation and Contractile Analysis of GFP-Sarcomere Reporter hiPSC-Cardiomyocytes.* Current protocols in human genetics, 2018. **96**: p. 21.12.1-21.12.12.
28. Rodriguez, M.L., et al., *Measuring the contractile forces of human induced pluripotent stem cell-derived cardiomyocytes with arrays of microposts.* Journal of biomechanical engineering, 2014. **136**(5): p. 051005-051005.
29. Sasaki, D., et al., *Contractile force measurement of human induced pluripotent stem cell-derived cardiac cell sheet-tissue.* PLOS ONE, 2018. **13**(5): p. e0198026.
30. Ribeiro, M.C., et al., *Functional maturation of human pluripotent stem cell derived cardiomyocytes in vitro--correlation between contraction force and electrophysiology.* Biomaterials, 2015. **51**: p. 138-150.
31. Saha, K., et al., *Surface creasing instability of soft polyacrylamide cell culture substrates.* Biophys J, 2010. **99**(12): p. L94-6.

32. Tuson, H.H., L.D. Renner, and D.B. Weibel, *Polyacrylamide hydrogels as substrates for studying bacteria.* Chemical communications (Cambridge, England), 2012. **48**(10): p. 1595-1597.
33. Caliari, S.R. and J.A. Burdick, *A practical guide to hydrogels for cell culture.* Nature methods, 2016. **13**(5): p. 405-414.
34. Kowalski, W.J., et al., *Quantification of Cardiomyocyte Alignment from Three-Dimensional (3D) Confocal Microscopy of Engineered Tissue.* Microsc Microanal, 2017. **23**(4): p. 826-842.
35. Paradis, A.N., M.S. Gay, and L. Zhang, *Binucleation of cardiomyocytes: the transition from a proliferative to a terminally differentiated state.* Drug discovery today, 2014. **19**(5): p. 602-609.
36. *anatomy and physiology - Cardiac Muscle Tissue*
37. LeGrice, I., A. Pope, and B. Smaill, *The Architecture of the Heart: Myocyte Organization and the Cardiac Extracellular Matrix*, in *Interstitial Fibrosis in Heart Failure*, F.J. Villarreal, Editor. 2005, Springer New York: New York, NY. p. 3-21.
38. Dusturia, N., et al., *Effect of myocardial heterogeneity on ventricular electro-mechanical responses: a computational study.* Biomedical engineering online, 2019. **18**(1): p. 23-23.
39. Dunn, G.A. and A.F. Brown, *Alignment of fibroblasts on grooved surfaces described by a simple geometric transformation.* J Cell Sci, 1986. **83**: p. 313-40.
40. Hu, J., et al., *Enhanced cell adhesion and alignment on micro-wavy patterned surfaces.* PloS one, 2014. **9**(8): p. e104502-e104502.
41. Asthana, A., et al., *Evaluation of cellular adhesion and organization in different microporous polymeric scaffolds.* Biotechnol Prog, 2018. **34**(2): p. 505-514.
42. Kane, R.S., et al., *Patterning proteins and cells using soft lithography.* Biomaterials, 1999. **20**(23-24): p. 2363-76.
43. Whitesides, G.M., et al., *Soft lithography in biology and biochemistry.* Annu Rev Biomed Eng, 2001. **3**: p. 335-73.
44. Kačarević, Ž.P., et al., *An Introduction to 3D Bioprinting: Possibilities, Challenges and Future Aspects.* Materials (Basel, Switzerland), 2018. **11**(11): p. 2199.
45. Chiu, D.T., et al., *Patterned deposition of cells and proteins onto surfaces by using three-dimensional microfluidic systems.* Proceedings of the National Academy of Sciences of the United States of America, 2000. **97**(6): p. 2408-2413.
46. Jeon, H., C.G. Simon, Jr., and G. Kim, *A mini-review: Cell response to microscale, nanoscale, and hierarchical patterning of surface structure.* J Biomed Mater Res B Appl Biomater, 2014. **102**(7): p. 1580-94.
47. Javaherian, S., K.A. O'Donnell, and A.P. McGuigan, *A fast and accessible methodology for micro-patterning cells on standard culture substrates using Parafilm™ inserts.* PloS one, 2011. **6**(6): p. e20909-e20909.
48. Cheng, Q., K. Komvopoulos, and S. Li, *Surface chemical patterning for long-term single-cell culture.* J Biomed Mater Res A, 2011. **96**(3): p. 507-12.
49. Kim, J.H., S. Seo, and J. Min, *Epithelial cell patterns on a PDMS polymer surface using a micro plasma structure.* J Biotechnol, 2011. **155**(3): p. 308-11.
50. Nakashima, Y., et al., *Creation of cell micropatterns using a newly developed gel micromachining technique.* Biofabrication, 2016. **8**(3): p. 035006.
51. Shrirao, A.B., et al., *A Versatile Method of Patterning Proteins and Cells.* Journal of visualized experiments : JoVE, 2017(120): p. 55513.
52. Albert, P.J. and U.S. Schwarz, *Modeling cell shape and dynamics on micropatterns.* Cell adhesion & migration, 2016. **10**(5): p. 516-528.
53. Martinez-Rivas, A., et al., *Methods of Micropatterning and Manipulation of Cells for Biomedical Applications.* Micromachines, 2017. **8**(12): p. 347.
54. Moeller, J., et al., *Controlling cell shape on hydrogels using lift-off protein patterning.* PloS one, 2018. **13**(1): p. e0189901-e0189901.
55. Freemont, A.J. and J.A. Hoyland, *Cell adhesion molecules.* Clinical molecular pathology, 1996. **49**(6): p. M321-M330.
56. Nishijima, K., et al., *The effects of cell adhesion on the growth and protein productivity of animal cells.* Cytotechnology, 2000. **33**(1-3): p. 147-155.
57. Ren, G., A.I. Roberts, and Y. Shi, *Adhesion molecules: key players in Mesenchymal stem cell-mediated immunosuppression.* Cell adhesion & migration, 2011. **5**(1): p. 20-22.
58. Veiseh, M., et al., *Short peptides enhance single cell adhesion and viability on microarrays.* Langmuir, 2007. **23**(8): p. 4472-9.
59. Hynes, R.O. and Q. Zhao, *The Evolution of Cell Adhesion.* The Journal of Cell Biology, 2000. **150**(2): p. 89-96.
60. Horwitz, A.R., *The origins of the molecular era of adhesion research.* Nature reviews. Molecular cell biology, 2012. **13**(12): p. 805-811.
61. Khalili, A.A. and M.R. Ahmad, *A Review of Cell Adhesion Studies for Biomedical and Biological Applications.* International journal of molecular sciences, 2015. **16**(8): p. 18149-18184.
62. Davidenko, N., et al., *Evaluation of cell binding to collagen and gelatin: a study of the effect of 2D and 3D architecture and surface chemistry.* Journal of materials science. Materials in medicine, 2016. **27**(10): p. 148-148.
63. Preissner, K.T. and D. Seiffert, *Role of vitronectin and its receptors in haemostasis and vascular remodeling.* Thromb Res, 1998. **89**(1): p. 1-21.
64. Pankov, R. and K.M. Yamada, *Fibronectin at a glance.* Journal of Cell Science, 2002. **115**(20): p. 3861-3863.
65. Boughton, B.J. and A.W. Simpson, *The biochemical and functional heterogeneity of circulating human plasma fibronectin.* Biochem Biophys Res Commun, 1984. **119**(3): p. 1174-80.
66. Jokinen, J., et al., *Integrin-mediated cell adhesion to type I collagen fibrils.* J Biol Chem, 2004. **279**(30): p. 31956-63.
67. Heino, J., *The collagen family members as cell adhesion proteins.* Bioessays, 2007. **29**(10): p. 1001-10.
68. Van Vlierberghe, S., et al., *12 - Porous hydrogel biomedical foam scaffolds for tissue repair*, in *Biomedical Foams for Tissue Engineering Applications*, P.A. Netti, Editor. 2014, Woodhead Publishing. p. 335-390.

69. Yue, K., et al., *Synthesis, properties, and biomedical applications of gelatin methacryloyl (GelMA) hydrogels.* Biomaterials, 2015. **73**: p. 254-271.
70. Nichol, J.W., et al., *Cell-laden microengineered gelatin methacrylate hydrogels.* Biomaterials, 2010. **31**(21): p. 5536-5544.
71. Han, L., et al., *Biohybrid methacrylated gelatin/ polyacrylamide hydrogels for cartilage repair.* Journal of Materials Chemistry B, 2017. **5**: p. 731-741.
72. Poncin-Epaillard, F., et al., *Surface treatment of polymeric materials controlling the adhesion of biomolecules.* Journal of functional biomaterials, 2012. **3**(3): p. 528-543.
73. Damodaran, V.B. and N.S. Murthy, *Bio-inspired strategies for designing antifouling biomaterials.* Biomater Res, 2016. **20**: p. 18.
74. Veronese, F.M., *Peptide and protein PEGylation: a review of problems and solutions.* Biomaterials, 2001. **22**(5): p. 405-17.
75. Cox, J.D., et al., *Surface passivation of a microfluidic device to glial cell adhesion: a comparison of hydrophobic and hydrophilic SAM coatings.* Biomaterials, 2002. **23**(3): p. 929-35.
76. Yu, Q., et al., *Anti-fouling bioactive surfaces.* Acta Biomater, 2011. **7**(4): p. 1550-7.
77. Bergstrand, A., et al., *Comparison of PEI-PEG and PLL-PEG copolymer coatings on the prevention of protein fouling.* J Biomed Mater Res A, 2009. **88**(3): p. 608-15.
78. Banerjee, I., R.C. Pangule, and R.S. Kane, *Antifouling coatings: recent developments in the design of surfaces that prevent fouling by proteins, bacteria, and marine organisms.* Adv Mater, 2011. **23**(6): p. 690-718.
79. Mizrahi, B., et al., *Long-lasting antifouling coating from multi-armed polymer.* Langmuir : the ACS journal of surfaces and colloids, 2013. **29**(32): p. 10087-10094.
80. Donahoe, C.D., et al., *Ultralow protein adsorbing coatings from clickable PEG nanogel solutions: benefits of attachment under salt-induced phase separation conditions and comparison with PEG/albumin nanogel coatings.* Langmuir : the ACS journal of surfaces and colloids, 2013. **29**(12): p. 4128-4139.
81. Lee, S. and J. Voros, *An aqueous-based surface modification of poly(dimethylsiloxane) with poly(ethylene glycol) to prevent biofouling.* Langmuir, 2005. **21**(25): p. 11957-62.
82. SuSoS. *PLL-g-PEG polymers*. 11-08-2019; Available from: https://susos.com/en/beschichtungstechnologien/pll-g-peg-polymere/.
83. Ruiz-Taylor, L.A., et al., *Monolayers of derivatized poly(L-lysine)-grafted poly(ethylene glycol) on metal oxides as a class of biomolecular interfaces.* Proceedings of the National Academy of Sciences of the United States of America, 2001. **98**(3): p. 852-857.
84. Azioune, A., et al., *Protein micropatterns: A direct printing protocol using deep UVs.* Methods Cell Biol, 2010. **97**: p. 133-46.
85. Johlin, J.M., *The Isoelectric Point of Gelatin in Relation to its "Minimum Physical Properties.".* Proceedings of the Society for Experimental Biology and Medicine, 1929. **26**(8): p. 702-704.
86. Terpilowski, K. and D. Rymuszka, *Surface properties of glass plates activated by air, oxygen, nitrogen and argon plasma.* Glass Physics and Chemistry, 2016. **42**(6): p. 535-541.
87. Mazia, D., G. Schatten, and W. Sale, *Adhesion of cells to surfaces coated with polylysine. Applications to electron microscopy.* The Journal of cell biology, 1975. **66**(1): p. 198-200.
88. Wang, G.X., et al., *The adhesive properties of endothelial cells on endovascular stent coated by substrates of poly-l-lysine and fibronectin.* Artif Cells Blood Substit Immobil Biotechnol, 2006. **34**(1): p. 11-25.
89. Gabi, M., et al., *Electrically controlling cell adhesion, growth and migration.* Colloids Surf B Biointerfaces, 2010. **79**(2): p. 365-71.
90. Desai, R.A., N.M. Rodriguez, and C.S. Chen, *"Stamp-off" to micropattern sparse, multicomponent features.* Methods Cell Biol, 2014. **119**: p. 3-16.